IN-46-CR
85168
P-55

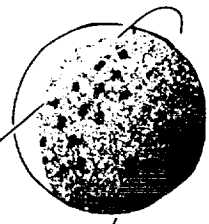

DETERMINATION OF CRUSTAL MOTIONS USING SATELLITE LASER RANGING

Final Report for NASA Grant NAG5-1118
February 15, 1989 - December 31, 1991

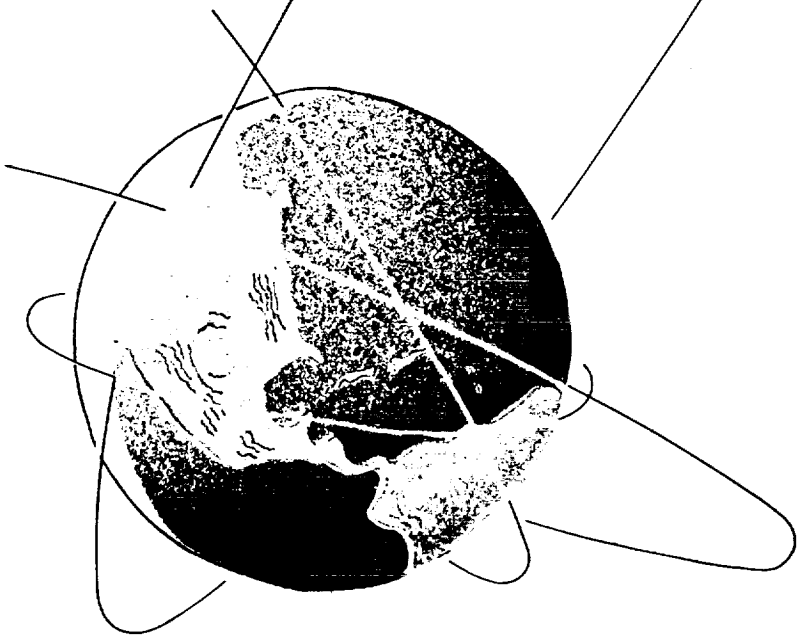

CENTER FOR SPACE RESEARCH

THE UNIVERSITY OF TEXAS AT AUSTIN AUSTIN, TEXAS

(NASA-CR-190246) DETERMINATION OF CRUSTAL MOTIONS USING SATELLITE LASER RANGING Final Report, 15 Feb. 1989 - 31 Dec. 1991 (Texas Univ.) 55 p CSCL 08G

N92-23540

Unclas
G3/46 0085168

Final Report for NASA Grant NAG5-1118:
"Determination of Crustal Motions Using Satellite Laser Ranging"
Center for Space Research
The University of Texas at Austin
Austin, TX 78712

INTRODUCTION

This report discusses the progress made under Crustal Dynamics Project funding by the University of Texas Center for Space Research on a wide variety of topics, including geodesy, geodynamics, and satellite dynamics. The report is derived from a manuscript submitted to the American Geopohysical Union Monograph dedicated to the Crustal Dynamics Project.

The ability to range accurately from the Earth's surface to satellites carrying laser cube-corner reflectors, along with the launching of the Lageos satellite in May 1976, has provided a unique capability for studying global solid Earth dynamics [Johnson et al., 1976]. During the period between Lageos launch through completion of the Crustal Dynamics Project at the end of 1991, the satellite laser ranging (SLR) technique has evolved into one of the fundamental geophysical and geodetic measurement techniques [Tapley et al., 1985; 1990, Frey and Bosworth, 1988]. The primary goals of the SLR system development and demonstration were to measure tectonic motion and Earth orientation. In the early 1980's, the technique achieved operational status in measuring Earth orientation and global baselines with the precision required to study plate motion and deformation. In addition, the technique has demonstrated unique abilities to measure both the constant and time-varying gravitational field properties of the Earth, to provide a unique terrestrial reference frame tied to the Earth's center of mass, and to study the dynamical effects of general relativity. It is currently regarded as a required tracking system for altimetric satellites such as TOPEX/POSEIDON and ERS-1.

The Lageos satellite, spherical in shape and covered with 426 corner cube reflectors, 422 of fused

silica for reflectance in the visible spectrum and 4 of germanium for infrared reflectance, was placed in a nearly circular orbit with an altitude of one Earth radius [Johnson et al., 1976; Cohen and Smith, 1985]. The combination of satellite design and orbit has provided an ideal ranging target for the SLR systems, which were originally developed in the 1960's, and have developed from meter level precision to the current subcentimeter level. The Lageos orbit provides a stable reference frame for studying the rotation of the Earth, the relative motion of points on the Earth's crust, and the time variation of the long-wavelength component of the Earth's gravity field. The Lageos orbit has a mean semimajor axis of 12,271 km, and eccentricity of 0.0044, and an inclination of 109.84° with respect to the Earth's equator. The orbit plane completes one rotation with respect to the true-of-date equinox in 1050 days in a prograde sense, while the perigee completes one revolution with respect to the Earth's equator in 1680 days in a retrograde sense. The satellite's altitude reduces the effects of uncertainties in the models for the high degree and order portion of the Earth's gravitational field and the effects of atmospheric drag. In addition, the satellite has a beryllium-copper core to increase its mass (407 kg) and a 60 cm diameter, thus giving the satellite a very small area-to-mass ratio of 6.95×10^{-4} m^2/kg. This further reduces the effect of difficult-to-model surface forces such as neutral and charged particle drag, radiation pressure, and thermal forces. The resulting orbit stability give the Lageos satellite a projected lifetime of over 500,000 years. Significant periods associated with the Lageos orbit are provided in Table 1.

Table 1. Significant Lageos Orbit Characteristics

Parameter	Period (days)
Orbital period	0.1566 (225 minutes)
Node period wrt inertial space	1050 (prograde)
Node period wrt Sun	560 (prograde)
Perigee period wrt inertial space	1680 (retrograde)

THE SLR GROUND NETWORK AND DATA SET

In the investigation described here, the University of Texas orbit analysis system, UTOPIA, was used to obtain a dynamically consistent solution to 15.1 years of Lageos laser range data. The data set spanned the period from May 7, 1976 to July 3, 1991, and included 561,708 normal points, constructed from two- and three-minute averages of the laser range observations from 117 different SLR sites. The single-shot ranging precision of the various systems varied from about a meter for some systems in 1976 to better than 10 mm for many of the systems at the end of the solution interval. The normal point precision is about an order of magnitude better. An important component of the tracking system coordinates is the offset, or eccentricity, between the laser site and the appropriate geodetic monument. These eccentricities are measured using ground surveying techniques with accuracies better than 1 cm. The eccentricity file used by UTCSR for this study was compared against a similar file maintained at the Goddard Spacefilght Center and indicated no significant discrepancies [Sellars, 1989]. The nominal epoch station coordinates used for this investigation were Lageos derived coordinates referred to as SSC(CSR)91L02. The solution approach is described by Watkins [1990]. The nominal plate motion model was the no net rotation absolute motion model AM0-2 of Minster and Jordan [1978]. The epoch for the plate motion was 1988.0.

As shown in Table 1, Lageos has a period of 225 minutes, providing 3–5 passes per day for most locations on the Earth. However, most stations attempt to acquire ranges for only the passes in a single 8-hour shift, which is usually scheduled during local nighttime. To reduce the computational burden, average or normal points are formed from the full-rate data collected by the station. These normal points are essentially average ranges over a selected duration, such as 2 or 3 minutes, and have been demonstrated to retain the geophysically and geodetically useful information of the full-rate data set [Smith et al., 1985; Tapley et al., 1985]. Normal points are used not only to relieve

computational effort but also to reduce the random or white noise content of the laser range measurements. The procedure accomplishes this by averaging a large number of raw ranges, and thus will not eliminate systematic errors which may be relatively constant or slowly varying over the two- or three-minute normal point window. The formation of the normal points used for this study follow the Herstmonceux recommendation outlined at the Fifth International Workshop (1984) on Laser Ranging Instrumentation. As Table 2 indicates, this approach has led to the set of 561,708 normal points which were used in this study. The mean precision for this set of 117 sites was 7.3 cm when averaged over the entire span, although many of the recent sites have average precisions of less than 1 cm.

Data Weighting

The quality and quantity of the Lageos range data has varied widely during the 15 years of the mission. The variation in data quality requires that a complex weighting algorithm be applied if the best estimates of the satellite orbit and geodetic parameters are to be obtained.

The data quality variation can be thought of as being of two types. The first type is the gradual increase in data quality with time as the laser instrumentation has improved. This is demonstrated by Figure 1, which plots the rms fit of normal points in 15-day arcs during the first 10 years of the mission, using the models described in the next sections. The resulting curve in Figure 1 was approximated with a four-part linear model with the following node points:

1976 (MJD 42905):	70 cm
1979 (MJD 44162):	40 cm
1983 (MJD 45578):	20 cm
1986 (MJD 47000):	12 cm

The weight of each normal point is linearly interpolated between the node points and is constant at the value of the last node point for times greater than the time of the last node.

The second type of variation in data quality is the variation from station to station within the network due to the variety of hardware systems in use at the tracking stations. This inhomogeneity is demonstrated by the results in Table 2. This table provides an estimate of the internal precision of each station in the network (column titled Prec. Est.), averaged over all data retained in the solution. This variation is modeled as a station dependent noise level which is added in an rms sense to the linear weighting described above. This correction was used only for those stations whose noise level is substantially higher than the network average at the time of operation of the site. In addition, recently occupied mobile sites are assigned slightly higher noise levels to reflect errors in nominal site positions. For this study, the systems were assigned the incremental noise levels in centimeters indicated in Table 2 (column titled Inc. Sig.). Stations with 0 in this column receive only the weighting assigned through the time dependent algorithm described above.

Table 2. SLR Station Performance
May 1976 – August 1991

Station		No. of Passes	No. of Obs.	Prec. Est (cm)	Inc. Sig. cm
1181	Pottsdam, Ger.	559	4048	9.1	30
1873	Simeiz, Uk.	82	590	7.3	100
1884	Riga, Lat.	121	794	6.9	100
1893	Katsively, Uk	41	304	4.6	100
1953	Santiago de Cuba, Cuba	106	532	8.4	100
7035	Otay Mt., USA	48	717	0.5	0
7046	Bear Lake, USA	45	651	3.6	10
7051	Quincy, USA	137	1271	6.0	0
7062	Otay Mt., USA	265	1958	2.9	0
7063	STALAS, GSFC, USA	446	4219	4.2	0
7065	GSFC, USA	3	19	8.3	0
7067	Bermuda	29	161	3.1	0
7068	Grand Turk, Bahamas	4	22	8.4	0
7080	McDonald Obs., USA	929	11369	1.0	0
7082	Bear Lake, USA	117	843	4.1	0
7084	Owens Val., USA	22	152	14.3	0
7085	Goldstone, USA	20	135	8.6	0
7086	Mcdonald Obs., USA	1270	13197	2.3	0
7090	Yaragadee, Aust.	3661	45811	1.9	0
7091	Haystack Obs., USA	412	3860	5.5	0
7092	Kwajalein	55	497	9.2	0
7096	American Samoa	124	953	6.7	0
7097	Easter Is., Ch.	198	2398	1.2	10
7100	GSFC, USA	5	41	6.7	0
7101	GSFC, USA	9	67	7.2	0

7102	GSFC, USA	229	2019	6.7	0
7103	GSFC, USA	60	578	4.8	0
7104	GSFC, USA	13	110	3.1	0
7105	GSFC, USA	1995	24343	0.8	0
7109	Quincy, USA	2652	38505	1.2	0
7110	Mon. Peak, USA	3129	41504	1.2	0
7112	Platteville, USA	624	6427	3.5	0
7114	Owens Val., USA	373	3316	3.5	0
7115	Goldstone, USA	379	3293	2.7	0
7120	Maui, USA	368	3460	2.1	0
7121	Huahine, Fr. Poly.	262	2125	3.1	0
7122	Mazatlan, Mex.	1356	17573	1.4	0
7123	Huahine, Fr. Poly.	179	2232	0.9	0
7125	GSFC, USA	35	325	1.7	0
7130	GSFC, USA	30	253	1.0	0
7210	Maui, USA	2084	23249	1.1	0
7220	Mon. Peak, USA	63	511	4.0	0
7236	Wuhan, PRC	52	678	2.6	60
7265	Mojave, USA	48	438	1.9	0
7274	Mon. Peak, USA	48	384	3.9	0
7288	Mojave, USA	185	2822	0.6	10
7295	Richmond, USA	86	1029	1.6	10
7400	Santiago, Ch.	42	339	2.3	10
7401	Cerra Tolola	222	3008	1.2	10
7403	Arequipa, Peru	150	2174	1.0	10
7510	Askites, Gr.	258	2589	2.0	10
7512	Rhodes, Gr.	176	1921	2.0	10
7515	Dionysos, Gr.	247	2969	2.1	10
7517	Roumeli, Gr.	225	2604	1.3	10
7520	Karitsa, Gr.	95	1052	2.1	10
7525	Xrisokellaria, Gr.	126	1570	0.9	10
7530	Bar Giyyora, Is.	97	920	4.5	30
7540	Matera, It.	32	225	1.4	10
7541	Matera, It.	61	535	1.9	10
7543	Noto, It.	49	529	1.4	10
7544	Lampedusa, It.	145	1577	2.0	10
7545	Cagliari, It.	120	1323	1.6	10
7546	Medicina, It.	11	85	2.3	10
7550	Bassovizza, It.	49	257	2.5	10
7575	Diyarbakir, Tur.	89	1183	1.6	10
7580	Melengiclic, Tur.	91	1227	0.4	10
7585	Yozgat, Tur.	84	909	2.0	10
7587	Yigilca, Tur.	83	1102	0.6	10
7596	Wettzell, Ger.	37	262	2.1	0
7597	Wettzell, Ger.	10	75	1.0	0
7599	Wettzell, Ger.	12	77	2.1	0
7602	Tromso, Nor.	45	405	2.7	10
7805	Metsahovi, Fin.	150	320	14.1	100
7810	Zimmerwald, Switz.	828	10510	2.3	10
7811	Borowicz, Pol.	99	639	7.3	100
7831	Helwan, Egy.	198	1794	1.7	30
7833	Kootwijk, Neth.	338	2399	11.7	30
7834	Wettzell, Ger.	1470	12809	1.8	10
7835	Grasse, Fr.	2717	41961	2.4	0
7837	Shanghai, PRC	256	2251	5.4	60
7838	Simosato, Jap.	1343	13857	2.9	10

7839	Graz, Aus.	1098	12992	0.9	0
7840	Greenwich Obs., UK.	3364	37127	1.8	0
7843	Orroral Val., Aust.	1535	15321	2.0	5
7853	Owens Val., USA	105	1743	2.0	0
7882	Cabo San Lucas, Mex.	54	641	0.6	0
7883	Ensenada, Mex.	35	273	0.6	0
7885	Mcdonald Obs., USA	34	218	1.6	0
7886	Quincy, USA	107	989	1.7	0
7888	Mt. Hopkins, USA	30	231	2.5	0
7891	Flagstaff, USA	36	281	2.8	0
7892	Vernal, USA	66	507	4.9	0
7894	Yuma, USA	45	221	2.6	0
7896	Pasadena, USA	66	516	3.1	0
7899	GSFC, USA	28	177	4.2	0
7907	Arequipa, USA	4046	46849	14.9	30
7918	GSFC, USA	53	619	0.4	100
7919	GSFC, USA	6	42	4.9	100
7920	GSFC, USA	25	230	0.5	100
7921	Mt. Hopkins, USA	686	6739	33.0	50
7929	Natal, Braz.	353	2152	31.1	50
7939	Matera, It.	2242	32328	5.3	20
7940	Dionysos, Gr.	3	15	9.7	100
7943	Orroral Val., Aust.	1381	14756	21.2	50
8833	Kootwijk, Neth.	106	1148	2.0	10
8834	Wettzell, Ger.	39	349	1.4	10
	TOTALS	48456	561708	7.3	

METHOD OF SOLUTION

Numerical Integration

The solution for the Lageos ephemeris, dynamic model parameters, and geodetic parameters was obtained by a weighted least squares batch estimation procedure which requires the solution of the differential equations governing the satellite's motion, as well as the state transition matrix for a defined period of satellite motion [Tapley, 1973]. For short arc solutions, this can be accomplished to a reasonable accuracy by numerically integrating the second order differential equations of the orbital motion in the form (Cowell's method)

$$\ddot{\vec{r}} = -\frac{\mu}{r^3}\vec{r} + \vec{f}(t, \vec{r}, \dot{\vec{r}}) \tag{1}$$

where $\vec{f}$ represents the perturbing forces to the two body motion. For the longer arcs described in this investigation, a modified Encke method was required to numerically integrate Eq. (1) [Lundberg

et al., 1991]. The numerical integration method for both the standard Cowell and modified Encke approaches was a Krogh-Shampine-Gordon 14^{th} order, fixed-step integrator described in Lundberg [1985]. The step size used was 300 seconds.

In UTOPIA, the dynamical equations which govern the motion of Lageos were expressed in an Earth-centered (non-rotating) cartesian coordinate frame, defined by the mean equator and equinox of epoch 2000.0 (J2000.0). This system is realized through the use of the JPL DE-200 planetary ephemeris, the 1976 International Astronomical Union (IAU) precession and the 1980 IAU Wahr nutation model. Corrections to the VLBI-determined IAU precession and nutation models [Herring, 1988] were also adopted. The orientation of the tracking stations (the body-fixed frame) relative to the celestial ephemeris pole of the Earth are provided through the use of the EOP(CSR)91L02 Earth orientation series [Eanes et al., 1991].

Long- and Short-Arc Solution Procedure

The determination of geophysical and geodetic parameters using Lageos laser range measurements at UTCSR involves a combination of long- and short-arc techniques [Tapley et al., 1985]. The long arc provides the starting point and is used primarily to study long-period perturbations in the Lageos orbit. The short arcs are constructed from the residuals of the long-arc orbit and form the basis for most geodetic work. A description of both techniques is provided in the specific context of the solutions determined for this study.

Long-Arc Solution

Using the data set described in Table 2 and a complete force and measurement model, a single, dynamically consistent trajectory was fit over the 15.1-year period from May 1976 through July 1991. The force and measurement models adhered largely to the IERS Standards, with the exception of the use of the TEG-2 mean gravity field developed at UTCSR, and the modelling of a signifcantly

more complete ocean and solid tide model, including ocean tide perturbations from over 80 constituents expanded to degree and order 20 where necessary, and third order solid tides [Tapley et al., 1991; Eanes et al., 1991; Casotto, 1989]. To achieve an accurate solution over this extended time interval, stringent demands must be met on the accuracy of the force models and computational software. The numerical integration process involves over 1.6 million steps in over 35,000 orbital revolutions, equivalent computationally to a 2700 year integration of the orbit of the Moon, a much more conservative dynamical system.

After converging the orbit through the entire data span in this manner, adjusting only the single set of Lageos initial conditions and 15 day along track accelerations, the range residual rms was 1.28 meters. The residuals from the long-arc solution were mapped into orbit elements using the UTCSR software package ELPSOL. A spectral analysis was carried out on the residual orbit element time series, and candidates for the sources of errors were identified and added to the adjusted parameter list on subsequent iterations to reduce the range residual rms.

Table 3. Contributions to 1.28 Meter Range Residual RMS By Individual Orbit Element

Element	Residual rms (m)
Semimajor Axis	0.002
Eccentricity	0.522
Inclination	0.127
Node	1.211
½ (ω + m)	0.498
½ (ω – m)	0.477

The dominant sources of error for each element shown in Table 3, were : semimajor axis – along-track acceleration variations with periods shorter than 15 days; eccentricity – odd zonal harmonics (constant + variability due to ocean tides and meteorological effects), and thermal surface effects (solar Yarkovsky + asymmetric albedo of spacecraft); inclination – ocean tide error dominated by K_1 and S_2; node – even zonal harmonics, particularly the secular variation $\dot{J}_2$, and periodic variability at

18.6 years and annual periods; periapse – odd zonal harmonic error (constant + variability), and thermal effects; along-track – variations in along-track "drag" as in semimajor axis. The linear combinations of periapse longitude and mean anomaly are used because they are more well suited for near circular orbits such as that of Lageos.

The second step in the long-arc procedure uses the 1.28 m orbit obtained by estimating only a small subset of parameters to tune a set of force model parameters in order to reduce the range residual rms. After adjusting the parameters described in Table 4 (for estimated ocean tides see Table 6), the range residual rms was reduced to 28 cm. It should be noted that solar reflectivity was not adjusted as a sub-arc parameter in the manner of the along-track acceleration, since previous studies at the Center for Space Research have indicated that the accuracy of the estimate of the reflectivity does not reach the 0.1% level of the hypothesized solar constant variability unless it is adjusted in intervals spanning several years [Willson and Hudson, 1988; Tapley et al., 1989]. This is due to the need for the shadowing function to decorrelate the powerful reflectivity parameter from other adjusted parameters.

Table 4. Estimated Parameter Summary

Parameter	Frequency
Initial conditions	Once
J_2, J_3	Once
$\dot{J}_2$	Once
Ocean tides	Once
Solar reflectivity	Once
Along-track acc.	15 days

Short-Arc Solutions

The 28 cm residuals from the final long arc fit were dominated by small model errors in ocean tide perturbations, including seasonal variability and thermal (Yarkovsky) forces [Eanes and Watkins, 1991]. Discussions of tide model errors including errors due to omission, commission, and to seasonal variability in the Lageos orbit are given by Eanes and Watkins [1991] and Casotto

Table 5. Contributions to 0.28 Meter Range Residual rms by Individual Orbit Element	
Element	Residual rms (m)
Semimajor Axis	0.001
Eccentricity	0.271
Inclination	0.066
Node	0.126
½ (ω + m)	0.259
½ (ω – m)	0.232

[1989]. The rms contribution of errors in each orbit element is presented in Table 5. These errors, because of both the magnitude and spectrum, can alias into the solutions for the geodetic parameters. The effects of long period force model errors must be removed from the residuals before an accurate solution for geodetic parameters can be obtained. The short-arc solution is designed to achieve this result, since the long period error can be accomodated in the estimate for the initial conditions in a manner similar to the classical variation of parameters approach used in celestial mechanics. The length of the short arcs were dependent on the data density and varied from 15 to 3 days according to:

1976 (MJD 42905) – 1979 (MJD 44162): 15 day
1979 (MJD 44162) – 1983 (MJD 45578): 6 day
1983 (MJD 45578) – 1989 (MJD 47585): 3 day

These cutoffs for the arc lengths were chosen to make the a posteriori uncertainties on the estimated orbit parameters more uniform over the data span [Watkins et al., 1989]. The Earth orientation parameters, station coordinates and other parameters of primary geodetic interest were adjusted simultaneously with the short-arc adjustments.

DYNAMICAL MODEL INVESTIGATIONS

As mentioned previously, the long arc technique is ideally suited to studying the accuracy of the dynamic models used to propagate the satellite orbit. If the dynamic model used to compute the

long-arc orbit is imperfect, the tracking data cannot be fit to the measurement precision, and systematic range residuals will result. By fitting the residuals with piecewise constant adjustments to the classical orbital elements over successive time intervals that are short with respect to the length of the long arc, a time series of the error in each orbital element is obtained. Spectral analysis of the time series provides a means of identifying what parts of the dynamical model need to be adjusted.

Gravitational Forces

Secular and Tidal Variations

Figure 2 shows an example of the above described process. The top panel shows the Lageos inclination residuals from May 1976 to July 1991 as computed using the nominal dynamical model with ocean tides fixed to the values from Schwiderski [1980]. Because errors in the dynamical model drive the derivatives of the orbital elements, a more direct comparison of the size of the model errors is obtained by analyzing the derivative of the orbital element time series. Figure 2c shows the derivative of the inclination residuals, the observed inclination excitations, and Figure 2d shows the power spectrum of these excitations. Peaks in the power spectrum at periods of 1050 days, 280 days, and 14.03 days are marked and labeled K_1, S_2 and M_2. These peaks show that there are errors in the nominal ocean tide model for these constituents. In particular this inclination signal points to the need to adjust the prograde degree 2 order 1 harmonic of the K_1 tide and the prograde degree 2 order 2 harmonics of the S_2 and M_2 tides.

Figure 2b shows the inclination residuals after these parameters (and others) have been adjusted using the Lageos data. The systematic signals are significantly reduced. The RMS of the inclination residuals about the best fitting line is 10 mas in Figure 2a and is 3 mas in Figure 2b. The slope of the remaining inclination residuals in Figure 2b is 0.3 mas/yr. The remaining signals, although substantially smaller, still indicate that further model improvement is possible.

Analysis of the other orbital element residual time series show that many other periodic signals exist that can be removed by adjusting tide parameters. Tables 6, 7, and 8 show the results of the adjustment of these tide parameters. The phase definition in these tables is adopted from that of Schwiderski [1980] as given in the IERS Standards [McCarthy et al., 1989].

The S_a tide, although not included in the 11 constituents computed by Schwiderski, can, nevertheless, be estimated from the other long period tides by assuming that the admittance of the ocean's response varies smoothly with frequency [Eanes et al., 1983; Christodoulidis et al., 1985]. Since S_a is a small term in the tidal potential the resulting estimate for the S_a tide parameters are also small. The Lageos values, however, are not small and clearly indicate that non-tidal sources of dynamical model error are present.

Table 6. Long Period Ocean Tide Solutions

	C_{20}^{+} cm	ε_{20}^{+} deg	C_{30}^{+} cm	ε_{30}^{+} deg	Source
S_a	2.17	23	11.4	282	Lageos (this paper)
	0.17	264	0.01	46	Schwiderski [1980]
	2.83	39	1.98	245	Starlette, Cheng et al. [1990]
S_{sa}	1.81	267	1.98	81	Lageos (this paper)
	1.24	222	0.06	2	Schwiderski [1980]
	1.59	253	0.78	69	Starlette, Cheng et al. [1990]
M_m	1.29	262	0.53	162	Lageos (this paper)
	1.06	259	0.06	94	Schwiderski [1980]
	1.42	246	-	-	Starlette, Cheng et al. [1990]
M_f	2.86	243	2.61	281	Lageos (this paper)
	1.70	252	0.19	148	Schwiderski [1980]
	2.84	242	-	-	Starlette, Cheng et al. [1990]

In the case of C_{20}^{+}, the estimate of the 2-cm S_a "ocean tide" is actually the result of seasonal redistribution of mass in the atmosphere and hydrosphere [Gutierrez and Wilson, 1987; Cheng et al., 1989; Chao and Au, 1991]. The 2-cm value for C_{20}^{+} is equivalent to an annual variation of J_2 with

Table 7. Diurnal Ocean Tide Solutions

	C_{21}^{+} cm	ε_{21}^{+} deg	C_{31}^{+} cm	ε_{31}^{+} deg	C_{41}^{+} cm	ε_{41}^{+} deg	Source
Q_1	0.72	314	0.08	297	0.48	281	Lageos (this paper)
	0.54	314	0.31	107	0.29	289	Schwiderski [1980]
	0.72	295	-	-	0.87	264	Starlette, Cheng et al. [1990]
O_1	2.46	308	0.91	64	1.77	301	Lageos (this paper)
	2.42	314	1.31	84	1.43	276	Schwiderski [1980]
	2.66	327	1.05	63	2.25	296	Starlette, Cheng et al. [1990]
P_1	0.85	323	0.47	48	-	-	Lageos (this paper)
	0.90	314	0.30	40	0.63	258	Schwiderski [1980]
	0.99	331	0.86	1	0.78	267	Starlette, Cheng et al. [1990]
S_1	0.14	328	1.12	232	-	-	Lageos (this paper)
	0.02	315	0.01	37	0.01	256	Schwiderski [1980]
K_1	2.47	326	1.31	31	-	-	Lageos (this paper)
	2.81	315	0.89	34	1.91	254	Schwiderski [1980]
	2.68	325	1.41	347	2.59	254	Starlette, Cheng et al. [1990]

an amplitude of 24×10^{-11}. The S_{sa} tide results also differ substantially from Schwiderski and are due to a semiannual variation of the mass distribution in the atmosphere and oceans. On the other hand, the 11.4 cm amplitude of S_a, represented by the value for C_{30}^{+}, is too large to be explained by mass transfer in the atmosphere. Since similar analysis using Starlette [Cheng et al., 1989] does not observe the same large signal, this anomaly indicates that there is some nongravitational term that needs correction in the Lageos dynamical model. In addition to the anomalous value of $S_a\, C_{30}^{+}$, the value of $S_1\, C_{31}^{+}$ obtained using the Lageos data is also large. These two anomalies are probably related and are discussed below.

The Lageos and Starlette results for $M_f\, C_{20}^{+}$ are both consistently larger than the Schwiderski value and show the same phase. The likely explanation is that both estimates are aliased by error in the nominal model for the fortnightly variation of UT1 [Yoder et al., 1981]. For Lageos, a 1-cm

Table 8. Semi-diurnal Ocean Tide Solutions							
	C_{22}^{+} cm	ε_{22}^{+} deg	C_{32}^{+} cm	ε_{32}^{+} deg	C_{42}^{+} cm	ε_{42}^{+} deg	Source
N_2	0.72	325	0.38	205	0.29	132	Lageos (this paper)
	0.65	322	0.11	172	0.21	142	Schwiderski [1980]
	0.92	329	-	-	0.13	148	Starlette, Cheng et al. [1990]
M_2	3.30	321.4	0.27	155	1.00	135	Lageos (this paper)
	2.96	310.6	0.36	169	1.00	125	Schwiderski [1980]
	3.22	319.3	0.12	161	1.15	121	Starlette, Cheng et al. [1990]
S_2	0.84	306	0.38	214	-	-	Lageos (this paper)
	0.93	314	0.26	202	0.37	103	Schwiderski [1980]
	0.83	302	0.23	192	0.32	89	Starlette, Cheng et al. [1990]
K_2	0.31	320	0.19	244	-	-	Lageos (this paper)
	0.26	315	0.09	195	0.11	104	Schwiderski [1980]
	0.29	316	0.08	243	0.10	97	Starlette, Cheng et al. [1990]

change in the amplitude of $M_f\, C_{20}^{+}$ corresponds to 0.02 ms or less than 2 percent of the total variation of UT1R-UT1. The causes of the large estimates of $M_m\, C_{20}^{+}$ and $M_f\, C_{30}^{+}$ are not known at this time.

In the diurnal tidal band, the results shown in Table 7 show that the satellite derived tide coefficients generally agree well with the oceanographic estimates from Schwiderski. The largest exception is the previously mentioned anomaly in $S_1\, C_{31}^{+}$. The 0.4 cm correction in the $K_1\, C_{21}^{+}$ coefficient is the source of the approximately 10 mas term in the Lageos inclination residuals shown in Figure 2. In terms of in-phase and out-of-phase parts of the K_1 tide, the Lageos result agrees with Schwiderski for the out-of-phase part ($C_{21}^{+} \cos \varepsilon_{21}^{+}$), but is 0.6 cm smaller for the in-phase part ($-C_{21}^{+} \sin \varepsilon_{21}^{+}$). The effect of changing the Earth's free core nutation (FCN) period from 460 days to 430 days as is indicated by analysis of nutation observations [Herring et al., 1991] should reduce the effective K_1 coefficient by 0.34 cm [Zhu et al., 1991], so the observed Lageos value is in better agreement with the smaller FCN period. Uncertainties in the actual ocean tide part of the K_1 signal

limits the usefulness of a more quantitative assessment of the FCN period deduced from the Lageos orbit analysis. The Starlette result from Cheng et al. [1990] is also more consistent with the lower FCN period.

In the semi-diurnal tide results given in Table 8, two interesting points can be noted. First, both the Lageos and Starlette analyses confirm that the Schwiderski value for M_2 degree 2 order 2 amplitude and phase requires a substantial correction. The out-of-phase part of this tide is $C_{22}^{+} \cos \varepsilon_{22}^{+}$ and is the largest contributor to the tidal deceleration of the Moon's mean motion [Cheng et al., 1992]. The contribution to the Moon's $\dot{n}$ based upon the Lageos M_2 result is -20.35 arcsec century^{-2}, while that due to the Starlette result is -19.27. The Schwiderski value gives -15.15. Results in Marsh et al. [1990] derived from a combination of satellites agree well with the Lageos value, and the higher energy disspation obtained by all of the satellite results matches the observed secular deceleration results from lunar laser ranging [Dickey et al., 1990] much better than the Schwiderski value. Also, both the Lageos and Starlette results for S_2 C_{22}^{+} and ε_{22}^{+} include the contribution of the atmosphere as discussed in Chapman and Lindzen [1970]; however, the difference between these results and those of Schwiderski are substantially smaller than the predicted atmospheric effect.

Although the adjustment of ocean tide parameters can remove many signals from the Lageos orbital element residuals, this parameterization can not handle the non-periodic variations of the low degree Stokes coefficients that are caused by non-tidal mass transfer in the atmosphere and oceans. Nor can they completely remove the effects of mismodeled nongravitational effects on Lageos.

The analysis of the residuals in the ascending node is shown in Figure 3. The large curvature of the residuals using the nominal dynamical model in Figure 3a is caused by a combination of unmodeled secular change in J_2 and an 18.6-year period variation due to uncertainties in the response on the inelastic Earth to long period tidal forces. The separation of these two effects, even

using more than 15 years of data, is still problematical due to extreme sensitivity of the results to unmodeled J_2 variability at frequencies of less than 0.2 cycles per year [Eanes and Watkins, 1991].

Leaving the issue of long period and secular variability of J_2 for further analysis, the node signals at frequencies greater that 0.2 cycles per year can be studied. Figure 3b shows the derivative of the node residuals of Figure 3a. Signals in this derivative, which will be referred to as the node excitation, are caused primarily by variations in J_2 and J_4 [Cheng et al., 1989]. Figure 3c shows the power spectrum of the time series of node excitations. The two largest peaks in the spectrum are labeled S_a and S_{sa} and represent annual and semiannual variability respectively. These anomalously large peaks are the source of the large adjustments of the degree 2 order 0 long period ocean tide coefficients discussed above. Although the semiannual peak is adequately removed by adjusting the S_{sa} ocean tide, many attempts at removing all of the annual power by adjusting the S_a tide fall short of this goal. The reason for this failure can be understood by the results, shown in Figures 3d and 3e, of a complex demodulation of the node excitation time series at the annual frequency followed by a bandpass filter. The results show that both the amplitude and the phase of the annual variation of J_2 show substantial interannual variability. The amplitude shows variations of ± 50 percent about the mean value of 100 mas year^{-1} and the phase changes by ± 30 degrees or about 1 month. The phase definition of Figure 3e is different from that of Table 3 by 93 degrees. A node excitation of 100 mas year^{-1} corresponds to an equivalent ocean tide amplitude of 1.98 cm or a J_2 variation of amplitude 24×10^{-11}.

The stochastic nature of the observed node excitation precludes the possibility of solving for parameters in a deterministic model of the J_2 variability. Future studies of the Lageos results to the predictions using meteorological data must go beyond comparisons of the mean annual and semiannual terms to test the coherence of the two time series at all frequencies. Preliminary results indicate that substantial coherence exists in the frequency range from 1 to 4 cycles per year

[Gutierrez et al., 1991; Eanes and Watkins, 1991].

The most puzzling feature of the orbital element residuals of the Lageos long arc is the large signal in eccentricity (e) and argument of perigee (ω). These two elements are closely related and for a nearly circular orbit a change of variables to the nonsingular pair, $e \cos \omega$ and $e \sin \omega$, simplifies the analysis [Yoder et al., 1983; Cheng et al., 1989]. The right-hand side of the differential equation for the complex quantity $\mathbf{P} = e \cos \omega - i\, e \sin \omega$ is referred to as the eccentricity vector excitation, Ψ_P. Variability in the odd zonal harmonics cause variations with the same spectrum in the real part of Ψ_P. Errors in the odd degree diurnal and semi-diurnal ocean tide coefficients of order 1 and 2 respectively cause variations in both the real and imaginary parts of Ψ_P.

Figures 4a and 4b show the real and imaginary parts of Ψ_P using the nominal dynamical model of the long arc. The real part of Ψ_P is dominated by an annual variation while the imaginary part is dominated by a variation with a period of 560 days, period of the S_1 tide perturbation and the interval of time required for one rotation of the Lageos orbital plane with respect to the Sun. These two features explain the anomalous estimates of the S_a C_{30}^{+} and S_1 C_{31}^{+} tide coefficients in Tables 3 and 4. But as mentioned above, the amplitudes of these terms are too large to be explained by tide effects alone, and Starlette analyses do not agree with these large values. This leads to the conclusion that this anomaly must be the result of a nongravitational acceleration of unknown origin acting on the Lageos orbit. The thermal imbalance and asymmetric albedo models (discussed later) that explain most of the observed Lageos drag-like acceleration and inclination slope do not seem to be adequate to remove the anomalous motion of the eccentricity vector. Until more is known about the source of the acceleration we must restrict ourselves to an empirical study which focuses on the form of the perturbations it causes.

More insight into the nature of these perturbations is achieved by the complex demodulation of the real part of Ψ_P shown in Figure 4c and 4d. The amplitude of the annual term has a mean of

70 mas year^{-1} corresponding to an equivalent ocean tide of 11 cm. From 1978 through 1987, this amplitude seems to decrease slightly and shows a modulation period of 3 years which is the beat period between the S_1 and S_a periods and which physically corresponds to the period of variation of the inclination of the Lageos node with respect to the ecliptic or the motion of the Lageos node with respect to the equinox (the K_1 period). In late 1988, a very large anomaly began which resulted in the amplitude tripling to more than 200 mas year^{-1} during 1989. More recent analysis indicates that the amplitude also reached this same level in 1991. The spectrum of Ψ_P indicates that the 560 day term in the imaginary part of Ψ_P also exists in the real part, and together they are equivalent to a prograde oscillation in Ψ_P with an amplitude of 40 mas year^{-1}. Radial or transverse accelerations in near resonance with the orbital motion of Lageos are required to explain these observed trends. The required amplitude of the once per revolution acceleration has a peak value of 200×10^{-12} m s^{-2} if it is in the transverse direction and twice this size if it is radial. This is about 1 percent as large as the direct solar radiation acceleration on Lageos. The eccentricity perturbations during the most anomalous year, 1989, reach 0.3×10^{-6}, corresponding to error in the radial component of the Lageos position of more than 3 meters. Note that short arc fits to the Lageos data will accommodate this effect into the adjustment of the orbit initial conditions and lead to a much reduced signal in the range residuals.

General Relativity

One of the factors to be considered in the analysis of precise laser ranging data is the inclusion of general relativity in the data reduction procedure. The relativistic treatment of the near- Earth satellite orbit determination problem involves relativistic equations of motion, corrections to the measurement model, and time transformations. The problem can be formulated in a solar system barycentric reference frame or a geocentric reference frame. As a result of the generalized principle of equivalence, the main relativistic effects on a near-Earth satellite should be due only to the

Schwarzschild field of the Earth itself [Ashby and Bertotti, 1984]. Analysis of laser range data to Lageos in both reference frames has verified that the geocentric frame is adequate for Earth satellite applications [Ries et al., 1988; Huang et al., 1990]. The modeling for the barycentric frame is described in Martin et al. [1985], but Ries et al. [1988] used Lageos range data to demonstrate that an additional correction to the relativistic barycentric equations of motion is necessary to properly model the oblateness of the Earth's gravitational field.

The largest dynamical effect of general relativity on a satellite orbit is the well-known precession of perigee. For Lageos, the perigee precession is approximately 9 mas/day, an effect easily observed in the Lageos perigee residuals if not modeled. Relativity theory also predicts several small effects, including a change in the mean motion of the satellite and a precession of the longitude of the node due to the angular momentum of the rotating Earth, the Lense-Thirring effect [Lense and Thirring, 1918]. In addition, there is a precession of the orbit plane due to the effect of geodesic (or de Sitter) precession [de Sitter, 1916]. This dynamical effect is not due to the Earth's mass, but rather to the motion of the Earth through the Sun's gravitational field. It is the result of the choice of a geocentric reference frame which is non-rotating with respect to the barycentric frame instead of a truly inertial geocentric reference frame, since the latter is difficult to realize in practice [Huang et al., 1990]. Observation of these small precessions by means of the analysis of the Lageos inclination and node residuals is presently not possible because of the uncertainties in the even zonal harmonics of the Earth's gravitational field. It has been proposed, however, that the effects of the uncertainties in the even zonals can be eliminated by placing a Lageos-type satellite in an orbit identical to Lageos but with an inclination supplementary to Lageos [Ciufolini, 1986, 1989, Tapley et al., 1989].

The Earth's Gravitational Coefficient

The value of the gravitational coefficient of the Earth (GM) is an important parameter in the determination of the scale of the coordinate system realized by satellite observations [Zielinski,

1981]. The best values of GM are generally accepted as those determined by observing the influence of this parameter on the motion of near-Earth satellites, and the satellite best suited for this purpose is the Lageos satellite. Lageos was designed to minimize the effects of nongravitational forces, and the gravitational effects of all but the longest wavelength components of the Earth's geopotential are greatly attenuated because of its high altitude. Thus the accuracy of the modeling of the forces on the Lageos satellite is more accurate than for any other satellite. In addition, the laser ranging measurements to Lageos are of very high accuracy.

In 1985, a solution for GM using only laser ranging to Lageos produced a value of $398600.434 \pm 0.002\ km^3/sec^2$ [Smith et al., 1985]. At the same time, a value for GM equal to $398600.440\ km^3/sec^2$ was determined from eight years of laser ranging to Lageos by UTCSR [Tapley et al., 1985]. The uncertainty in the UTCSR estimate was reported subsequently as $0.002\ km^3/sec^2$ [Chovitz, 1987]. More recently, UTCSR reported a solution for GM obtained from a 3-year fit to Lageos laser ranging, and also from a multi-satellite solution, to be $398600.4405 \pm 0.001\ km^3/sec^2$ [Ries et al., 1989]. The relativistic effects appropriate to the geocentric frame were modeled, where the coordinate time is equivalent to the current definition of Terrestrial Dynamical Time (TDT) [Huang et al., 1990].

In the initial determination, the Lageos laser range data were processed with a small but significant error in one of the range corrections. Optical tests on the Lageos-II satellite, which was built by the Agenzia Spatiale Italiana (ASI) to be a replica of the Lageos satellite, prompted a review of the tests conducted on Lageos. It was discovered that the value for the correction for the offset between the Lageos center-of-mass and the effective reflecting surface should be about 251 mm [Fitzmaurice et al., 1977] rather than the adopted 240 mm value [McCarthy, 1989]. In a new UTCSR determination of GM using the corrected center-of-mass offset, a value of $398600.4415\ km^3/sec^2$ in TDT units has been obtained, with an estimated uncertainty (1-σ) of

0.0008 km^3/sec^2 [Ries et al., 1992].

While the direct effects of general relativity were taken into account in the data analyses described above, there is an indirect effect on the units being used that must be considered. The primary effect of general relativity on time is that coordinate time in different reference frames may run at different rates. Because the International Astronomical Union (IAU) definition of the time coordinate of the solar system barycentric reference system requires that only periodic differences exist between Barycentric Dynamical Time (TDB) and TDT, the spatial coordinates in the barycentric frame have effectively been rescaled [Misner, 1982; Hellings, 1986; Guinot and Seidelmann, 1988]. Thus the value of GM would be 398600.4418 km^3/sec^2 in SI units and 398600.4356 km^3/sec^2 in TDB units. Recommendations have been made to modify the IAU definition for coordinate times to eliminate the rescaling, which would result in the units of length remaining SI units in all reference frames [Guinot, 1991].

Nongravitational Forces

The dominant nongravitational force on Lageos is radiation pressure. The radiation may come directly from the Sun, it may be sunlight reflected by the Earth, or it may be infrared radiation that is emitted by the Earth. Temperature imbalances on the satellite itself can lead to 'photon thrusts'. Finally, there is expected to be some atmospheric drag even at the altitude of Lageos. Other forces, such as perturbations by the Earth's magnetic field, interplanetary dust, the solar wind, or Poynting-Robertson drag, are not expected to have significant effects on the Lageos orbit [Rubincam, 1982; Ciufolini, 1989].

Solar and Earth Radiation Pressure

Although the shape of the Lageos satellite is simple, modelling the effect of radiation pressure directly from the Sun is not trivial. A conical shadow model (umbra and penumbra) for the Earth

and Moon is generally used, but the numerical integration step-size is usually much larger than the duration of partial shadowing, and the effect is essentially a discontinuity in the solar radiation pressure force. Implementation of a procedure to more accurately account for the effect of shadowing is underway [Feulner, 1990]. While some orbit error may be attributable to the current method of integrating across the shadow boundary, experiments varying integrator step-size and shadow radius indicate that this is not the cause of the anomalous along-track accelerations observed in the Lageos orbit.

It is unclear how much the modelling of the effects of Earth radiation pressure have benefitted the Lageos long arc fits. The effects are significant, and it has been possible to estimate the average reflectivity of the Earth from a Lageos long-arc, but it is likely that the orbital effects could be absorbed to some degree by other dynamical model parameters. The UTCSR model for Earth radiation pressure numerically integrates the heat and diffusely reflected sunlight from the visible disk of the Earth [Knocke et al., 1988]. The average and seasonal variations in the Earth's albedo and infrared emission are included in a second-degree zonal representation. The temporal and geographic variations of the Earth's albedo are expected to depart considerably from the zonal averages, so, at best, the Earth radiation pressure model only represents the long period effects. It is possible that some of the short period variations in the Lageos along-track acceleration are due to sunlight reflected diffusely and specularly by the Earth [Anselmo et al., 1983].

Surface Forces and the Lageos Spin Vector

After subtracting most of the known forces acting on the Lageos satellite, there still remained a significant along-track acceleration which reduces the semi-major axis by approximately 1 mm per day. The mean values of the anomalous acceleration (or drag) determined every 15 days by UTCSR for the first 14.1 years of the previously discussed data set are plotted in Figure 5. The mean of the acceleration over the entire arc is about 3.5 picometer sec^{-2} with fluctuations that are sometimes as

large as the mean. The largest variations (spikes) occur when Lageos is experiencing eclipsing of the Sun by the Earth, although every eclipsing interval does not necessarily generate a spike. Thus both the mean and the variations required explanation.

Earth Yarkovsky

A thermal drag model, a variant of the Yarkovsky effect, has been proposed by Rubincam [1987, 1988] which is able to account for much of the observed average along-track acceleration. The infrared radiation from the Earth is absorbed by the laser retroreflectors, and, because Lageos is spinning rapidly, the heat distribution is uniform longitudinally but not latitudinally. This creates a temperature imbalance between the Lageos northern and southern hemispheres, generating a thrust along the spin axis as the heat is re-radiated. The proposed thermal drag model accounts for about 70% of the observed drag, and the remainder most likely consists of a combination of neutral particle drag and charged particle drag [Rubincam, 1990]. This model also predicts periodic variations about the mean with frequencies of once and twice per node revolution of the Lageos orbit (1050 and 525 day periods).

The effect of thermal drag due to Earth heating was simulated for the first 12.4 years of the Lageos mission. The 15-day averages of the accelerations generated by the nominal Rubincam [1988] model, augmented by 1 picometer sec^{-2} to account for neutral and charged particle drag, compared well with the observed accelerations if the spikes were ignored. It was noted, however, that the modeled drag diverged from the observed drag in the last part of the 12.4 year arc in both amplitude and phase The deviation appeared to suggest that the spin axis of Lageos is evolving from its original orientation (where the agreement between the nominal model and observed drag is good) and becoming aligned with the Earth's poles. A similar conclusion is reached by Rubincam [1990]. Rubincam [1987] suggested that the spin axis of the Lageos satellite should eventually align itself with the Earth's spin axis. This has been confirmed by Bertotti and Iess [1991], who have analyzed

the effect of gravitational and magnetic torques on the satellite as the eddy current dissipation reduces the spin rate. In the UTCSR model, a model for the spin axis evolution was determined empirically so that the thermal drag fits the observed drag better. In Figure 6, it can be seen that the modified model is able to maintain good agreement in amplitude and phase of the periodic variation throughout the 12.4 year arc. A few direct measurements of the actual Lageos spin vector are clearly needed, since this effect, and the effects described below, depend strongly on the orientation of the spin axis.

Examination of the orbit inclination residuals provide additional evidence supporting the thermal drag model. In the UTCSR Lageos long arcs where the thermal drag was not modeled, the residual errors in the orbit inclination have exhibited a slope of 1.3 to 1.5 mas year^{-1}. The slope in the Lageos inclination residuals had been a concern, since there seemed to be no reasonable force which could generate this particular signal. The effect of a co-rotating atmosphere at Lageos altitude was considered, but it was found that even if one assumed that 100% of the drag was atmospheric drag, a co-rotating atmosphere could account for less than 10% of the inclination slope. By incorporating the 'Earth Yarkovsky' model in the latest long arc, the inclination slope is only 0.3 mas year^{-1}. It is convincing to note that the thermal drag model is able to explain much of the average drag, the variation at the 1050 and 525 day periods, and most of the peculiar inclination slope. If the magnitude of the thermal drag force was increased to about 90% of the observed drag, then the remaining inclination slope would be explained also. Any other explanation for the inclination slope is still unknown.

Solar Yarkovsky

A similar thermal thrust mechanism, due to heating by the sun, has been proposed to account for at least part of the large spikes that occur only during eclipse seasons [Rubincam, 1982; Slabinski, 1988; Afonso et al., 1989; Scharroo et al., 1991; Ries et al., 1991]. Since the spin axis orientation is

essentially fixed with respect to the Sun during an orbit, the hemisphere of the Lageos satellite which is experiencing summer (tilted towards the sun) will be warmer than the opposite hemisphere at every point in the orbit. Ignoring the Earth's heat and the effect of shadowing, this temperature difference will be essentially constant, and there is no significant net effect on the orbit. During shadowing, however, the solar thermal force does not average out, and there is a net along-track acceleration.

A model for this effect was included in the force model for Lageos, and the estimated drag was compared to the observed drag. The maximum magnitude of the 'Solar Yarkovsky' acceleration (80 picometer sec^{-2}) was empirically chosen to give peaks with amplitudes comparable to the observed drag. Afonso et al. [1989] and Scharroo et al. [1991] independently analyzed the expected surface temperatures and arrived at accelerations with similar magnitudes. The spin axis orientation in the UTCSR model was based on the modified spin axis model when calculating the 'season' for each hemisphere. Unfortunately, it has not been possible to choose a set of parameters for this model which could predict the correct series of peaks.

Asymmetric Reflectivity

An additional mechanism is proposed that, when combined with the Solar Yarkovsky effect, appears to account for the spikes observed during the eclipse seasons. If it is assumed that the two halves of the satellite do not have the same effective reflectivity, then there will be an asymmetry in the solar radiation pressure on the satellite that, averaged over the spin period, will be along the direction of the spin vector. Like the solar Yarkovsky effect, there is no significant orbital effect except during eclipse seasons. The cause of the reflective asymmetry is not known. Scharroo et al. [1991] speculates that the two halves of the satellite may have been finished differently and finds that the northern hemisphere of Lageos need only be 1/70th more specular than the southern one. Ries et al. [1991] suggests that the non-symmetrical distribution of the infrared corner-cubes may be the

cause. There are three infrared cubes in the southern hemisphere and only one in the northern hemisphere, and since they appear opaque at optical wavelengths, the northern hemisphere is likely to be more reflective than the southern hemisphere. Whatever the source of the asymmetry, augmenting the thermal forces with an imbalance in the reflectivity leads to a model that is capable of generating the accelerations similar to those observed on the Lageos satellite over the first 12.4 years as shown in Figure 7. The agreement, however, is still not perfect, which illustrates that the models are still deficient in some respects.

Lageos Spin Vector

As the Lageos spin vector evolves with time, the models described above may become less reliable. Analysis of the along-track accelerations estimated in the latest Lageos long-arc, which incorporated the UTCSR surface force models described above, indicates that the agreement after the first twelve years is degrading. It is critical for the modeling of these surface forces that measurements of the spin axis orientation are obtained. Eventually, however, the spin rate will slow enough to result in chaotic behavior. When this occurs, it is not clear whether the thermal forces will average out and thus be attenuated, or become more significant and more difficult to model.

DEFINITION OF THE TERRESTRIAL REFERENCE FRAME

Using the short arc adjustments as discussed earlier enables not only an improved fit to the laser ranges as measured by range residual rms, but also allows a frequency domain separation of orbit error from kinematic effects in the residuals, namely those due to the positions of the ground tracking sites. These sites, being tied to the surface of the Earth, are forced to have a diurnal variation in the inertial frame. In the satellite frame, the variation differs from once per revolution by one cycle per sidereal day a signal which is easily detectable and separable from other effects. The most significant remaining orbit error at this frequency is due to error in the order 1 geopotential

coefficients, but the effect is considerably smaller than that of the kinematic signal of the site position errors at the few millimeter level when averaged over many revolutions.

The rigid rotations of the tracking network, that is, that part of the site motions common to all the sites in rotation, are, by definition, polar motion and Earth rotation, collectively referred to as Earth orientation parameters (EOP). Clearly, if both the complete tracking network and all EOP's are adjusted simultaneously, a singularity results, and the arbitrary orientation of the network aliases into the EOP's. This problem is solved primarily by adjusting the network positions once over a relatively long span of time while adjusting the EOP's frequently, such as once per day. Under these restrictions, only the mean values of the EOP series are inseparable from the orientation of the network. This last singularity is generally removed by the application of one of several types of constraints, including the fixing of specific fiducial site(s), or the fixing of EOP's on one reference day [Smith et al., 1991; Robertson et al., 1990]. An alternative method is to apply an analytic constraint equation that forces the "net rotation" of the tracking network adjustments with respect to a nominal set to be zero, and they are thus absorbed by the EOP series [Bender and Goad, 1979]. Such a constraint allows continuity of the combined tracking network and EOP series, referred to as the terrestrial reference frame (TRF), over time as more data from additional sites is acquired. The implementation of this method is under study at UTCSR, although for the present, an ad hoc realization of this approach is used by constraining through a priori covariance both the EOP and tracking sites. This covariance is chosen to be sufficiently loose to allow short period variation in the EOP's without allowing long-term variations or drift. For the results presented in this paper, the a priori uncertainty on each site coordinate was 1 meter, 10 mas on x and y pole position, and 0.7 ms on UT1. A priori correlations were set to zero. By not fixing any single site, the terrestrial reference frame is freed from the vagaries, in either data quality or quantity, of a particular site.

The estimation of UT1 using SLR, or any satellite technique, is complicated by the fact that long period modeling of the motion of the longitude of the ascending node of the orbit(s) is at present impossible due to the stochastic variation in the mass distribution of the atmosphere, and to unmodelled surface forces. The relative size of these perturbations depend upon tha satellite design and orbit characteristics. For Lageos, the variability in zonal mass distribution is the more significant. Thus, UTCSR currently produces UT1 estimates which are constrained to a VLBI solution at long periods, but which are increasing independent as the frequency increases. This technique was first described in Robertson et al. [1983], using a Gaussian filter with full width at half maximum of 90 days, and yielded rms agreement of 0.7 ms. By contrast, using an improved Vondrak smoothing technique tying to JPL SPACE90 [Gross et al., 1991], and greatly improved observations and analyses from both techniques, the rms agreement in 1990 was less than 0.07 ms [IERS Ann. Rep., 1990].

Inclusion of Site Velocities

When the span of observations becomes long enough, site velocities may need to be estimated, particularly for sites in deforming regions where the a priori plate model may not be accurate. The inclusion in the adjusted parameter set of site velocities adds an additional singularity to the above discussion, namely that between the mean slope in the EOP's and the net rotation rate derived from the combined velocities of the sites in the TRF. This is resolved in an analogous manner to that described above, through fixing fiducial velocities, two reference EOP days, or explicit constraint equations. The current implementation at UTCSR involves constraint through a priori covariance, and through the adjustment only of those sites with considerable velocity departures from the nominal Minster and Jordan AM0-1 velocity [Minster and Jordan, 1978]. Alternatively, many sites can be adjusted, and the resulting EOP series can be detrended with respect to an a priori series for continuity. This approach is used when many sites velocities are adjusted for studies of global

tectonics.

Site Position, Velocity, and Earth Orientation Solutions from UTCSR

With the above introduction as background, the several types of solutions for geodetic parameters produced at UTCSR can be discussed. The first type of solution is performed annually and represents an updated version of the UTCSR TRF. This solution spans the entire Lageos mission from 1976 through the end of the reporting year, and adjusts mean site coordinates, velocities for selected sites, and a time series of EOP's, most recently using 3 day resolution. Since the series is reported to the International Earth Rotation Service and forms a significant portion of the combined IERS EOP series and International Terrestrial Reference Frame (ITRF), it is important that these series be expressed in a well defined reference frame, and hence not all sites, even those with sufficient data, have adjusted velocities. In the most recent such solution, SSC(CSR)91L03, seven sites in tectonically deforming regions had velocity adjustments: 7110 Monument Peak (USA), 7109 Quincy (USA), 7838 Simosato (Japan), 7939 Matera (Italy), 7907 Arequipa (Peru), 7097 Easter Island (Chile), and 7123 Huahine (French Polynesia).

The EOP series associated with this solution are analyzed for the combined IERS series by the IERS Central Bureau at the Paris Observatory. For the 1990 report, the EOP(CSR)91L03 series was assessed at roughly the 0.6 mas level in x and y polar motion, and 0.07 ms in UT1, for the period 1986-1990 [IERS Annual Report, 1991]. This was among the most accurate of any series reported that year. A typical polhode of recent polar motion as determined from UTCSR Lageos and IRIS VLBI is presented in Figure 8. The considerable progress made by all space geodetic techniques is evident when the history of such intercomparisons is recalled. Robertson et al. [1983] presents 5 mas agreement in pole position between UTCSR SLR and IRIS VLBI. Robertson et al. [1985] presents agreement during 1984–1985 of 2 mas in pole position. Comparisons in BIH and IERS annual reports from 1986 to 1990 trace the accuracies to their current submilliarcsecond level.

Interestingly, Carter et al. [1984] also presented one of the first comparisons of EOP derived from space geodetic techniques and that predicted from measurements of atmospheric angular momentum (AAM), and demonstrated clearly the significant El Niño event of 1983 and associated peak in excess length of day. The seasonal discrepancy between space geodetic measurements and AAM was also noted, and it was correctly conjectured to be largely due to the effects of the atmosphere (stratosphere) above 50 mb.

A second type of solution produced on an annual basis adjusts all sites and velocities (with sufficient data) for the basis of assessing global tectonic models. Roughly 30–40 sites have strong velocity solutions [Watkins et al., 1989; Smith et al., 1991]. Relative motions for sites in Europe derived from such solutions is presented in Figure 9. Alternatively, to test internal consistency of the site solutions, independent solutions of few month duration can be determined for each site, and the velocities inferred from these time series [Watkins, 1990]. Such a solution for the baseline length between Monument Peak, CA, on the Pacific plate, and Quincy, CA, on the North American plate is presented in Figure 10. The slope of the best fit line is the well known –25 mm/yr adjustment with regard to the RM2 predicted velocity, and the rms scatter about the best fit line of 7 mm is remarkably small for such a long observation period.

The accuracy of the epoch site coordinates can best be measured through comparison with an independent technique with collocated observations. A careful comparison of SLR solutions computed at UTCSR and VLBI solutions computed at GSFC for sites occupied primarily in 1988 resulted in rms agreements of 15, 21, and 22 mm in x, y, and z, respectively [Ray et al., 1990]. These numbers include the uncertainties in each solution and the uncertainties in the survey ties connecting the observing monuments of each technique. Analysis of the chi-square per degree of freedom indicated that each techniques formal uncertainties should be scaled by approximately 2, resulting in uncertainties of less than 10 mm in each component for the best observed sites. An extension of the

Ray et al. paper analyzing the results of site positions determined using significantly more data, and requiring mapping with estimated velocities for both techniques is presented by Himwich et al. [this issue].

By computing successive seven parameter transformations between the several month solutions and the nominal TRF, the translational origin or geocenter position can be determined. The most significant proposed source of motion between the solid Earth, on which the tracking sites reside, and the center of mass of the solid Earth-atmosphere-hydrosphere is mass redistribution in the ocean. Figure 11 demonstrate the geocenter history in 15 day intervals since 1987. The rms about the mean is 12 mm in X, 9 mm in Y, and 25 mm in Z. The source of the long period trend in X is unclear, but it is statistically significant (rms after removal of best fit line is 9 mm), and may represent true long period geocenter motion. Full analyses of the geocenter time series is the subject of a forthcoming manuscript.

A third type of solution is performed each week, and is referred to as the UTCSR Earth Orientation Rapid Service. This service involves the gathering of recent Lageos data, and the computation of the EOP's in near real time, and provides prompt reports to the United States Naval Observatory and the IERS for their rapid service Bulletins A and B. This solution has been performed and reported weekly since 1982. Site coordinates in this operational service are held fixed to the values from a previous annual solution and not readjusted, hence the EOP's from the operational service are perhaps a few tenths of a milliarcsecond less accurate than those of the annual solutions.

Future Improvements to SLR Derived Geodetic Parameters

A number of improvements lie on the horizon for the determination of geodetic parameters using the SLR technique. The first of these is improved temporal resolution of EOP's obtained through Kalman filtering of the orbit parameters. Because the SLR data are obtained each day, although

some days may be sparse, information on the orbit and geodetic parameters is available on a daily basis, although some knowledge of the spectral power of the unmodeled orbit excitations and high frequency EOP excitation is required for optimal performance. The improved temporal resolution of the space geodetic EOP series, which may also be possible with the use of GPS, will aid in the understanding of momentum exchange between the components of the Earth system, particularly between the atmosphere and solid Earth, at short periods. Although a manuscript on the application of Kalman filtering of the Lageos orbit and the resulting high frequency EOP series is in preparation, preliminary results are presented in Figure 12, which demonstrates the UTCSR Lageos 1 day x and y pole positions plotted with GSFC processing of the high density, high quality VLBI ERDE (Extended Research and Development Experiment) period in the fall of 1989. Both series are differenced from a smoothed Lageos nominal series. The overall rms agreement in each coordinate is 0.7 mas, although slightly better during the heart of the campaign (October). In addition, determination of the diurnal and semidiurnal variations in EOP's induced primarily by ocean tides has been demonstrated at the 20 microarcsecond level or better through analysis of a recent span of high quality Lageos data from 1987–1991 [Watkins et al., 1991].

Another exciting development is the use of additional geodetic satellites such as Lageos-2 and the Soviet Etalon-1 and Etalon-2. Lageos-2, an identical twin of the current Lageos-1, will be launched in fall 1992 into an orbit similar to that of Lageos-1 but with an inclination of 52 degrees. Assuming adequate tracking is available for both satellites, the use of observations to both satellites in a simultaneous solution can reduce the time on site for SLR systems by approximately a factor of two while retaining the same accuracy as currently obtained. The Etalon spacecraft, launched into orbits of the Glonass spacecraft, similar to those of the Global Positioning System, can also provide reduced time on site, but can also assist in the extension of the period over which the SLR derived UT1 estimates can remain independent from those of VLBI. This is made possible by the

attenuation at the Etalon altitude of the stochastic variations in even zonal harmonics of the Earth's gravity field which drive the satellite node. The response of the nodal longitudes of the Etalon spacecraft is roughly 10 times less to a given excitation in even zonal harmonics than those of Lageos-1 or Lageos-2. Thus the current limit of approximately 50 days over which SLR can obtain independent measurements of UT1 may be extended considerably.

CONCLUSIONS

Satellite laser ranging has matured over the last decade into one of the essential space geodesy techniques. It has demonstrated centimeter site positioning and millimeter per year velocity determinations in a frame tied dynamically to the mass center of the solid Earth-hydrosphere-atmosphere system. Such a coordinate system is a requirement for studying long term eustatic sea level rise and other global change phenomena. Earth orientation parameters determined with the coordinate system have been produced in near real time operationally since 1983, at a relatively modest cost. The SLR ranging to Lageos has also provided a rich spectrum of results based upon the analysis of Lageos orbital dynamics. These include significant improvements in the knowledge of the mean and variable components of the Earth's gravity field and the Earth's gravitational parameter, The ability to measure the time variations of the Earth's gravity field has opened as exciting area of study in relating global processes, including meteorologically derived mass transport through changes in the satellite dynamics. Finally, new confirmation of General Relativity has been obtained using the Lageos SLR data.

With the launching of Lageos-2 and Lageos-3, the future decade holds significant promise for substantially improving the accuracy and applicability of the SLR technique.

ACKNOWLEDGEMENTS

Additional computing resources provided by the University of Texas Center for High

Performance Computing.

REFERENCES

Afonso, G., F. Barlier, M. Carpino, P. Farinella, F. Mignard, M. Milani, and A. M. Nobili, Orbital effects of Lageos seasons and eclipses, *Ann. Geophys. A, 7*(5), 501–514, 1989.

Anselmo, L., B. Bertotti, P. Farinella, A. Milani, and A. M. Nobili, Orbital perturbations due to radiation pressure for a spacecraft of complex shape, *Celest. Mech., 29*, 27, 1983.

Ashby, N., and B. Bertotti, Relativistic perturbations of an Earth satellite, *Phys. Rev. Let., 52*, 485–488, 1984.

Bender P.L. and C. Goad, The Use of Artificial Satllites for Geodesy and Geodynamics, vol. 2, pp.145-161, 1979.

Bertotti, B., and L. Iess, The rotation of Lageos, *J. Geophys. Res., 96*, 2431–2440, 1991.

Carter W. E., D. S. Robertson, J. E. Pettey, B. D. Tapley, B. E. Schutz, R. J. Eanes, and Miao Lufeng, *Science, 224*, pp. 957-961, 1984

Casotto, S., Ocean Tide Models for TOPEX Precise Orbit Determination, Ph.D. Dissertation, Department of Aerospace Engineering and Engineering Mechanics, The University of Texas at Austin, Austin, Texas, 1989.

Chao, B. F., and A. Y. Au, Temporal variation of the Earth's low-degree zonal gravitational field caused by atmospheric mass redistribution: 1980–1988, in press, *J. Geophys. Res.,* 1991.

Chapman S., and R. S. Lindzen, *Atmospheric Tides: Thermal and Gravitational*, Gordon and Breach, New York, 1970

Cheng, M. K., R. J. Eanes, C. K. Shum, B. E. Schutz, and B. D. Tapley, Temporal variations in low degree zonal harmonics from Starlette orbit analysis, *Geophys. Res. Lett., 16*(5), 393, 1989.

Cheng, M. K., C. K. Shum, R. J. Eanes, B. E. Schutz, and B. D. Tapley, Long Period Perturbation in Starlette Orbit and Tide Solution, *J. Geophys. Res., 95*(B6), 8723–8736, 1990.

Cheng, M. K., R. J. Eanes, and B. D. Tapley, Tidal Deceleration of the Moon's Mean Motion, *Geophys. J. Int.*, in press, 1992.

Chovitz, B. H., Parameters of common relevance of Astronomy, Geodesy and Geodynamics, Report of the IAG Special Study Group 5:100, XIX General Assembly of IUGG, Vancouver, August 1987.

Christodoulidis, D. C., D. E. Smith, R. Kolenkiewicz, S. M. Klosko, M. H. Torrence, and P. J. Dunn, Observing tectonic plate motions and deformations from satellite laser ranging, *J. Geophys. Res., 90*(B11), 9249–9263, 1985.

Christodoulidis, D. C., D. E. Smith, R. G. Williamson, and S. M. Klosko, Observed tidal braking in the Earth/Moon/Sun system, *J. Geophys. Res., 93*(B6), 6216, 1988.

Ciufolini, I., Measurement of the Lense-Thirring drag on high-altitude, laser-ranged artificial satellites, *Phys. Rev. Let., 56,* 278, 1986.

Ciufolini, I., A comprehensive introduction to the Lageos Gravitomagnetic Experiment, *Int. J. Mod. Phys. A, 4*, 3083, 1989.

Coates, R. J., H. Frey, J. Bosworth, and G. D. Mead, Space Age Geodesy: The NASA Crustal Dynamics Project, *IEEE Trans., GE-23*, 1985.

Cohen, S. C., and D. E. Smith, Lageos scientific results: Introduction, *J. Geophys. Res., 90*, 9217–9220, 1985.

de Sitter, W., On Einstein's theory of gravitation and its astronomical consequences, *Mon. Not. R. Astron. Soc., 77,* 155, 1916.

Dickey, J. O., X X Newhall, and J. G. Williams, Investigating relativity using lunar laser ranging: Geodetic precession and the Nordvedt effect, JPL Geodesy and Geophysics Preprint, *No. 173*,

Pasadena, California, March 1989.

Dickey J. O., J. G. Williams, and X. X. Newhall, The Impact of lunar laser ranging on geodynamics, *Eos Trans. AGU*, 71(17),475, 1990

Eanes, R. J., B. D. Tapley, and B. E. Schutz, Earth and ocean tide effects on Lageos and Starlette, *Proceedings of the Ninth International Symposium on Earth Tide*, J. T. Kuo, ed., E. Schweizerbart'sche Verlagsbuchhandlung, 1983.

Eanes, R. J., and M. M. Watkins, Temporal variability of Earth's gravitational field from satellite laser ranging observations, XX General Assembly of the IUGG, IAG Symp. No. 3, Vienna, Austria, August 1991.

Eanes, R. J., M. M. Watkins, and B. E. Schutz, contribution to IERS Annual Rep. for 1990, Paris Obs., 1991.

Feulner, M. R., The Numerical Integration of Near-Earth Satellite Orbits Across SRP Boundaries Using the Method of Modified Back Differences, CSR-TM-90-03, Center for Space Research, The University of Texas at Austin, Austin, TX 78712, August 1990.

Fields, R. K., Long Arc Orbit Determination Improvements Using Encke's Method, Master's Thesis, Department of Aerospace Engineering and Engineering Mechanics, The University of Texas at Austin, Austin, Texas, 1988.

Fitzmaurice, M. W., P. O. Minott, J. B. Abshire, and H. E. Rowe, Prelaunch Testing of the Laser Geodynamics Satellite (Lageos), NASA Technical Paper 1062, October 1977.

Frey, H. V. and J. M. Bosworth, Measuring Contemporary Crustal Motions: NASA's Crustal Dynamics Project, *Earthquakes and Volcanoes, 20*, 3, 1988.

Gross R., and ..., contribution in IERS Annual Rep. for 1990, Paris Obs., 1991.

Guinot, B. and P. K. Seidelmann, Time scales: Their history, definition and interpretation, *Astron. Astrophys., 194*, 304–308, 1988.

Guinot, B., Report of the Sub-Group on Time, *Proc. 127th Colloquium of the International Astronomical Union, Reference Systems*, J. Hughes, C. Smith and G. Kaplan (eds.), United States Naval Observatory, 1991.

Gutierrez, R., and C. R. Wilson, Seasonal air and water mass redistribution effects on Lageos and Starlette, *Rev. Geophys. Space Phys., 21*(8), 1657, 1987.

Gutierrez, R., R. J. Eanes, M. K. Cheng, and C. R. Wilson, Global air mass redistribution effects on the laser geodetic satellites, Lageos and Starlette, submitted to *J. Geophys. Res.*, 1991.

Hellings, R. W. , Relativistic effects in astronomical timing measurements, *Astron. J., 91*(3), 650–659, 1986.

Herring, T. A., Resolutions to IAU nutations working group, personal communication to D. McCarthy, July 14, 1988.

Herring T. A., B. A. Buffett, P. M. Mathews, and I. I. Shapiro, Forced Nutations of the Earth: Influences of Inner Core Dynamics, 3. Very Long Baseline Interferometry Data Analysis, *J. Geophys. Res.*, 96(B5), 8259–8273, 1991

Huang, C., J. C. Ries, B. D. Tapley, and M. M. Watkins, Relativistic Effects for Near-Earth Satellite Orbit Determination, *Celest. Mech., 48*, 167–185, 1990.

International Earth Rotation Service (IERS), *Annual Report for 1990*, Central Bureau of IERS – Observatoire de Paris, 61 avenue de l'Observatoire, F-75014 Paris, France, June 1991.

Johnson, C. W., C. A. Lundquist, and J. L. Zuransky, The Lageos Satellite, Presented at the International Astronautical Federation XXVIIth Congress, Anaheim, CA, October 1976.

Knocke, P., J. C. Ries, and B. D. Tapley, Earth Radiation Pressure Effects on Satellites, in Proc. AIAA/AAS Astrodynamics Conference, Minneapolis, Minnesota, August 15P17, 1988.

Lense J., and H. Thirring, ber die Einfluss der Eigenrotation der Zentralkorper auf die Bewegung der Planeten und Monde nach der Einsteinchen Gravitationstheorie, *Phys. Zeitschr.*, 19, 156, 1918;

English translation by B. Mashhoon et al., *Gen. Relativ. Grav.*, 16, 711, 1984.

Lundberg, J. B., Computational Errors and Their Control in the Determination of Satellite Orbits, CSR-85-3, Center for Space Research, The University of Texas at Austin, Austin, Texas, 1985.

Lundberg, J. B., B. E. Schutz, R. K. Fields, and M. M. Watkins, The Application of Encke's Method to Long Arc Orbit Determination Solutions, *AIAA Journal of Guidance, Control, and Dynamics, 14*(3), 683–686, May-June 1991.

Marsh, J. G., F. J. Lerch, B. H. Putney, D. C. Christodoulidis, D. E. Smith, T. L. Felsentreger, B. V. Sanchez, S. M. Klosko, E. C. Pavlis, T. V. Martin, J. W. Robbins, R. G. Williamson, O. L. Colombo, D. D. Rowlands, W. F. Eddy, N. L. Chandler, K. E. Rachlin, G. B. Patel, S. Bhati, and D. S. Chinn, A new gravitational model for the Earth from satellite tracking data: GEM-T1, *J. Geophys. Res., 93*(B6), 6169, 1988.

Marsh J.G. and 12 others, The GEM-T2 Gravitational Model, *J. Geophys. Res.*, 95, 22043–22071, 1990.

Martin, C. F., M. H. Torrence, C. W. Misner, Relativistic effects on an Earth-Orbiting satellite in the barycenter coordinate system, *J. Geophys. Res., 90*, 9403–9410, 1985.

McCarthy, D. D. (ed.), *IERS Standards (1989)*, IERS Technical Note 3, Central Bureau of IERS – Observatoire de Paris, November 1989.

Minster, J. B., and T. H. Jordan, Present-day plate motions, *J. Geophys. Res., 83*(B11), 5331, 1978.

Misner, C. W., Scale Factors for Relativistic Ephemeris Coordinates, EG&G Washington Analytical Services Center, NASA contract NAS5-25885 report, 1982 (unpublished).

Newhall, X X, E. M. Standish, and J. G. Williams, DE 102, a numerically integrated ephemeris of the Moon and planets spanning forty-four centuries, *Astron. Astrophys., 125,* 150, 1983.

Ray, J. R., J. W. Ryan, C. Ma, T. A. Clark, B. E. Schutz, R. J. Eanes, M. M. Watkins, and B. D. Tapley, Comparison of VLBI and SLR Geocentric Site Coordinates, submitted to *Geophys. Rev.*

Lett., 1990.

Ries, J. C., C. Huang, and M. M. Watkins, Effect of General Relativity on a near-Earth satellite in the geocentric and barycentric reference frames, *Phys. Rev. Lett., 61,* 903–906, 1988.

Ries, J. C., R. J. Eanes, C. Huang, B. E. Schutz, C. K. Shum, B. D. Tapley, M. Watkins, and D. N. Yuan, Determination of the gravitational coefficient of the Earth from near-Earth satellites, *Geophys. Res. Lett., 16*(4), 271, 1989.

Ries, J. C., R. J. Eanes, and M. M. Watkins, The along-track acceleration of Lageos, *Eos Trans. AGU, 72*, 17, Supplement p. 95, 1991.

Ries, J. C., R. J. Eanes, C. K. Shum, and M. M. Watkins, Progress in the determination of the gravitational coefficient of the Earth, submitted to *Geophys. Res. Lett.*, 1992.

Robertson D. S., W. E. Carter, R. J. Eanes, B. E. Schutz, B. D. Tapley, R. W. King, R. B. Langley, P. J. Morgan, and I. I. Shapiro, Comparison of Earth rotation as inferred from radio interferometric, laser ranging, and astrometric observations, *Nature*, 302(5908), 509–511, 1983.

Robertson D. S., W. E. Carter, B. D. Tapley, B. E. Schutz, and R. J. Eanes, Polar Motion Measurements: Subdecimeter Accuracy Verified by Intercomparison, *Science*, 229, 1259–1261, 1985.

Robertson D. S., and others, contribution to IERS Annual Rep. for 1990, Paris Obs., 1991.

Rubincam, D. P., On the secular decrease in the semimajor axis of Lageos's orbit, *Celest. Mech., 26*(4), 361, 1982.

Rubincam, D. P., Lageos orbit decay due to infrared radiation from the Earth, *J. Geophys. Res., 92*(B2), 1287, 1987.

Rubincam, D. P., Yarkovsky thermal drag on Lageos, *J. Geophys. Res., 93*(B11), 13805, 1988.

Rubincam, D. P., Drag on the Lageos satellite, *J. Geophys. Res., 95*, 4881–4886, 1990.

Scharroo, R., K. F. Wakker, B.A.C. Ambrosius, and R. Noomen, On the along-track acceleration of the Lageos satellite, *J. Geophys. Res., 96*, 729–740, 1991.

Sellars, P., Personal communication, 1989.

Schutz, B. E., M. K. Cheng, C. K. Shum and R. J. Eanes,

and B. D. Tapley, Analysis of Earth rotation solution from Starlette, *Journal of Geophysical Research, 94*(B8), 10,167–10,174, August 1989.

Schwiderski, E. W., On charting global ocean tides, *Rev. Geophys. Space Phys., 18,* 243–268, 1980.

Slabinski, V. J., Lageos acceleration due to intermittent solar heating during eclipse periods, in proceedings of 19th Regular Meeting of Division on Dynamical Astronomy – American Astronomical Society, Gaithersburg, Maryland, July 25–26, 1988.

Smith D. E., R. Kolenkiewicz, P. J. Dunn, S. M. Klosko, M. H. Torrence, S. K. Fricke, and S. Blackwell, A global geodetic reference frame from Lageos ranging (SL5.1AP), *J. Geophys. Res.*, 90(B11), 9221–9233, 1985.

Smith D. E., R. Kolenkiewicz, P. J. Dunn, J. W. Robbins, M. H. Torrence, S. M. Klosko, R. G. Williamson, E. C. Pavlis, N. B. Douglas, and S. K. Fricke, Tectonic Motion and Deformation From Satellite Laser Ranging to LAGEOS, *J. Geophys. Res.*, 95(B13), 22013–22042, 1991.

Tapley, B. D, Statistical orbit determination theory, *Recent Advances in Dynamical Astronomy*, D. Reidel Publishing Co., 396–425, 1973.

Tapley, B. D., B. E. Schutz, and R. J. Eanes, Station coordinates, baselines, and Earth rotation from Lageos laser ranging: 1976–1984, *J. Geophys. Res., 90*(B11), 9235–9248, 1985.

Tapley, B. D., B. E. Schutz, and R. J. Eanes, Satellite Laser Ranging and Its Applications, *Cel. Mech.*, 37, 247–261, 1985.

Tapley, B. D., Geophysical parameter determination using satellite ranging, *Proceedings of International Symposium on Problems in Astronautics and Celestial Mechanics in Memory of*

Giuseppe Colombo, Turin, Italy, in press, June 10–12, 1987.

Tapley, B. D., and J. C. Ries, Orbit determination requirements for TOPEX, *Proceedings of AAS/AIAA Astrodynamics Specialist Conference*, Paper No. 87-429, Kalispell, Montana, August 10–13, 1987.

Tapley, B. D., J. C. Ries, M. M. Watkins, R. J. Eanes, Simulation of an Experiment to Measure the Lense-Thirring Precession Using a Second Lageos Satellite, Appendix A of the NASA/University of Texas Lageos-3 Feasibility Study, B. D. Tapley and I. Ciufolini, Eds., September 1989.

Tapley, B. D., B. E. Schutz, R. J. Eanes, and M. M. Watkins, Contributions of Satellite Laser Ranging to Geodesy and Geodynamics, *Adv. Space Res.*, 1991.

Tapley, B. D., C. K. Shum, D. N. Yuan, J. C. Ries, R. J. Eanes, and M. M. Watkins, The University of Texas Earth Gravitational Field Model (TEG-2), XX General assembly of the IUGG, Vienna, Austria, Aug. 1991. Proceedings to be published, 1992.

Wahr, J. M., Body Tides on an Elliptical, Rotating, Elastic and Oceanless Earth, *Geophys J. R. Astron. Soc., 64*,677, 1981.

Watkins, M. M., R. J. Eanes, and B. D. Tapley, Stations and Plate Motions from Lageos Long Arc LLA8903, proceedings of the 125^{th} Anniversary Meeting of the International Association of Geodesy, Edinburgh, Scotland, August 1989.

Watkins, Tracking Station Coordinates and Their Temporal Evolution as Determined From Laser Ranging to the Lageos Satellite, Ph.D. dissertation, The Univ. of Texas at Austin, May 1990.

Watkins M. M., B. E. Schutz, and R. J. Eanes, High Frequency Monitoring of Earth Orientation Parameters Using Lageos and GPS, *EOS Trans. AGU*, 72(44), 120, 1991.

Willson, R. C., and H. S. Hudson, Solar luminosity variations in solar cycle 21, *Nature, 332*, 810, 1988.

Yoder, C. K., J. G. Williams and M. E. Parke, Tidal variations of Earth rotation, *J. Geophys. Res.*, *86*(B2), 881–891, 1981.

Yoder, C. F., J. G. Williams, J. O. Dickey, B. E. Schutz, R. J. Eanes, and B. D. Tapley, Secular variations of Earth's gravitational harmonic J_2 coefficients from Lageos and nontidal acceleration of Earth rotation, *Nature, 303,* 757, 1983.

Zhu S. Y., E. Groten, and C. Riegber, Various Aspects of Numerical Determination of Nutation Constants. II. An Improved Nutation Series for the Deformable Earth, *Ast. J.*, 99(3), 1990.

Zielinski, J. B., Origin and scale of coordinate systems in satellite geodesy, *Reference Coordinate Systems for Earth Dynamics*, E. M. Gaposhkin and B. Kolaczek (eds.), 239–250, D. Reidel, Dordrecht, 1981.

Doctoral Degrees Supported by this Grant (1988-1991)

Cheng, M.K., Time Variations in the Earth's Gravity Field from Starlette Orbit Analysis, Ph.D, The University of Texas, 1988.

Knocke, P. Earth Radiation Pressure Effects on Satellites, Ph.D, The University of Texas, 1989.

Watkins, M. M., Tracking Station Coordinates and Their Temporal Evolution as Determined from Laser Ranging to the Lageos Satellite, Ph.D., The University of Texas, 1990.

Fig. 1. Evolution of the laser ranging network tracking Lageos from 1976 to 1991.

Fig. 2. Analysis of inclination residuals from Lageos Long Arc 9107. (a) Residuals using the nominal dynamical model. (b) Residuals after adjusting dynamical model parameters. (c) First derivative of the residuals in (a). (d) Power spectrum of the time series in (c).

Fig. 3. Analysis of longitude of the ascending node residuals from Lageos Long Arc 9107. (a) Residuals using the nominal dynamical model. (b) First derivative of the residuals in (a). (c) Power spectrum of the time series in (b). (d) Amplitude and (e) phase of the annual variation obtained by complex demodulation of the time series in (b).

Fig. 4. Analysis of the eccentricity vector excitation residuals from Lagesos Long Arc 9107. The (a) real and (b) imaginary parts of the eccentricity vector excitation (Ψ_P). The (c) amplitude and (d) phase of the annual variation of the real part of Ψ_P obtained by complex demodulation of the time series in (a).

Fig. 5. Observed along-track acceleration for Lageos.

Fig. 6. Modified Earth Yarkovsky model compared to observed along-track acceleration during the first 12.4 years of the Lageos mission.

Fig. 7. Combined models for Earth and Solar Yarkovsky, asymmetric reflectivity and atmospheric drag compared to observed accelerations.

Fig. 8. Polar motion obtained from UTCSR Lageos and IRIS VLBI, 1987-89.

Fig. 9. Baseline rates

Fig. 10. Variability of the baseline length from Monument Peak to Quincy, 1982-90.

Fig. 11. Estimates of the translations along the x, y, and z axes of the instantaneous origin of the terrestrial reference system with respect to the geocenter, 1987-91.

Fig. 12. Kalman smoothed polar motion at a 1-day resolution from Lageos compared to GSFC VLBI results during the 1989 ERDE Campaign.

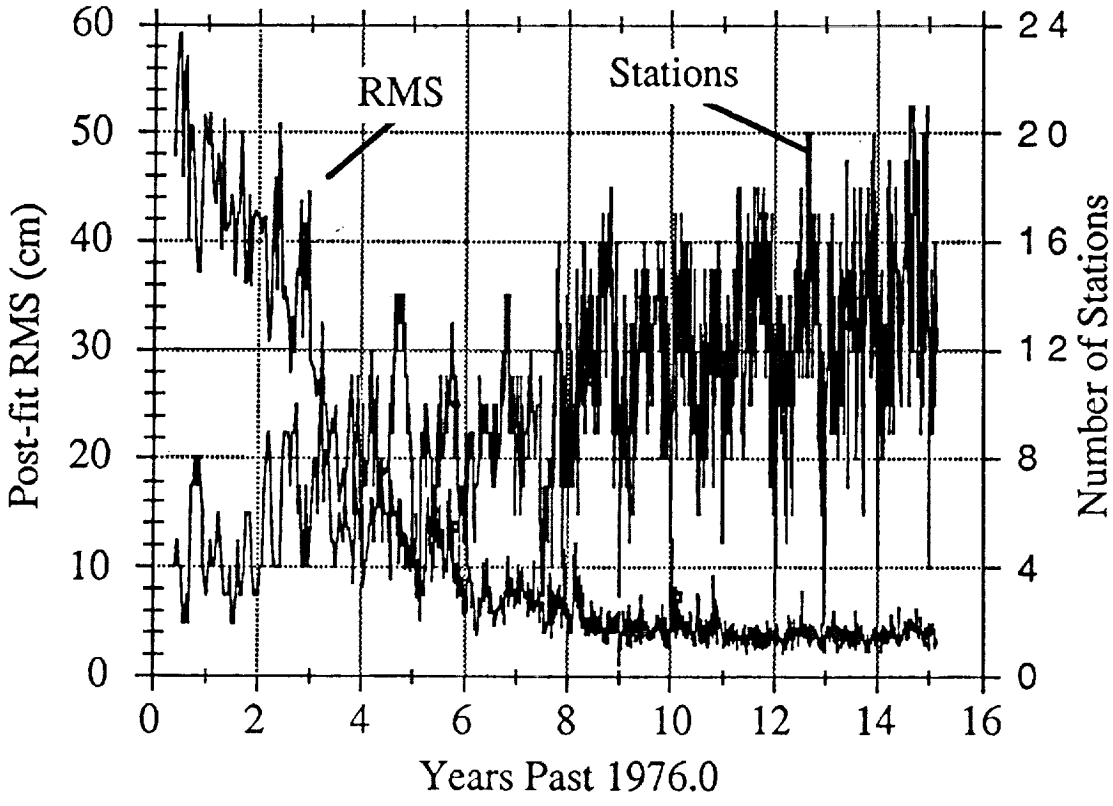
RMS
Stations
Post-fit RMS (cm)
Number of Stations
Years Past 1976.0
0
10
20
30
40
50
60
0
4
8
12
16
20
24
0
2
4
6
8
10
12
14
16

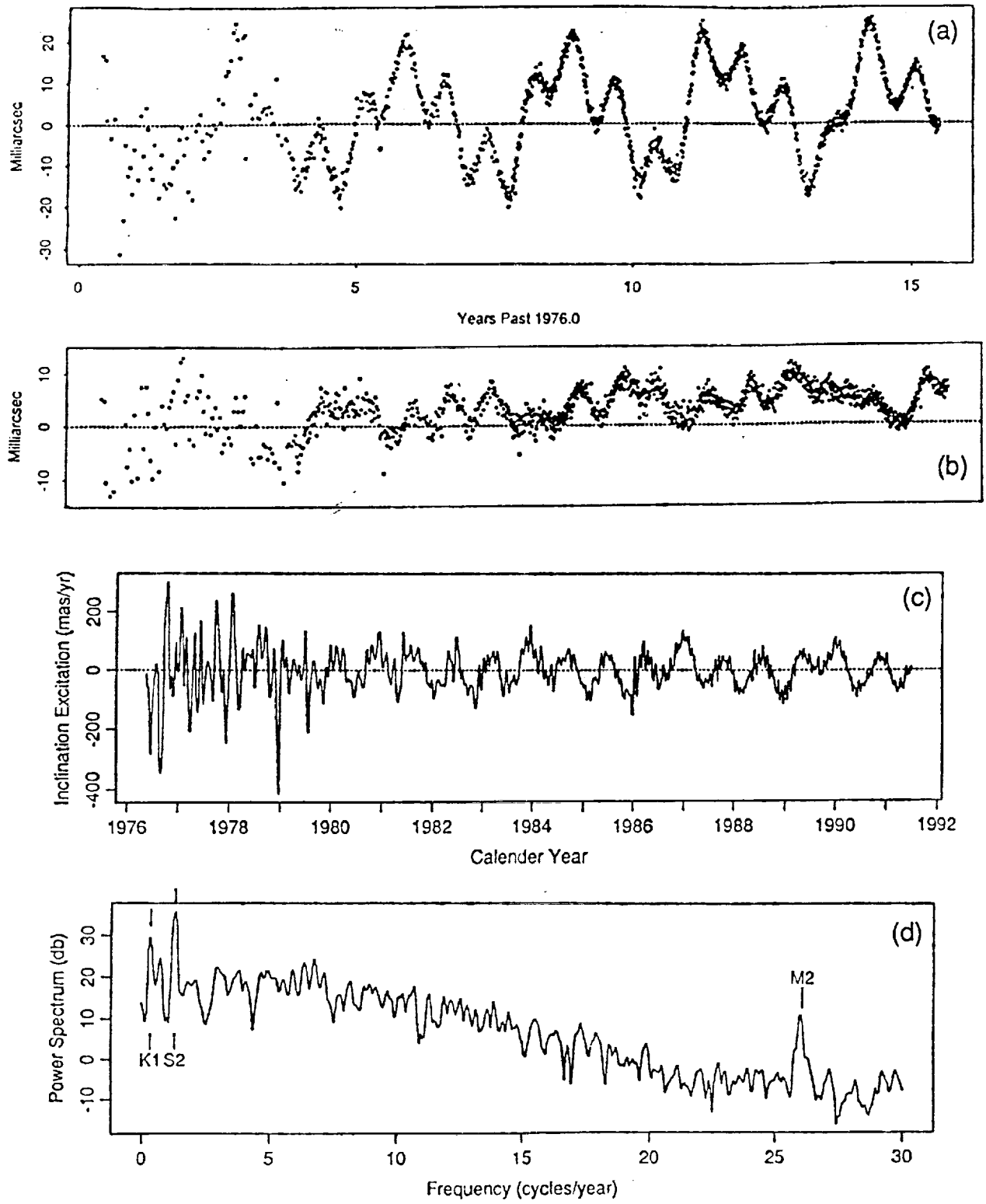
(a)
Milliarcsec
20
10
0
-10
-20
-30
0
5
10
15
Years Past 1976.0
(b)
Milliarcsec
10
0
-10
(c)
Inclination Excitation (mas/yr)
200
0
-200
-400
1976
1978
1980
1982
1984
1986
1988
1990
1992
Calender Year
(d)
Power Spectrum (db)
30
20
10
0
-10
K1
S2
M2
0
5
10
15
20
25
30
Frequency (cycles/year)

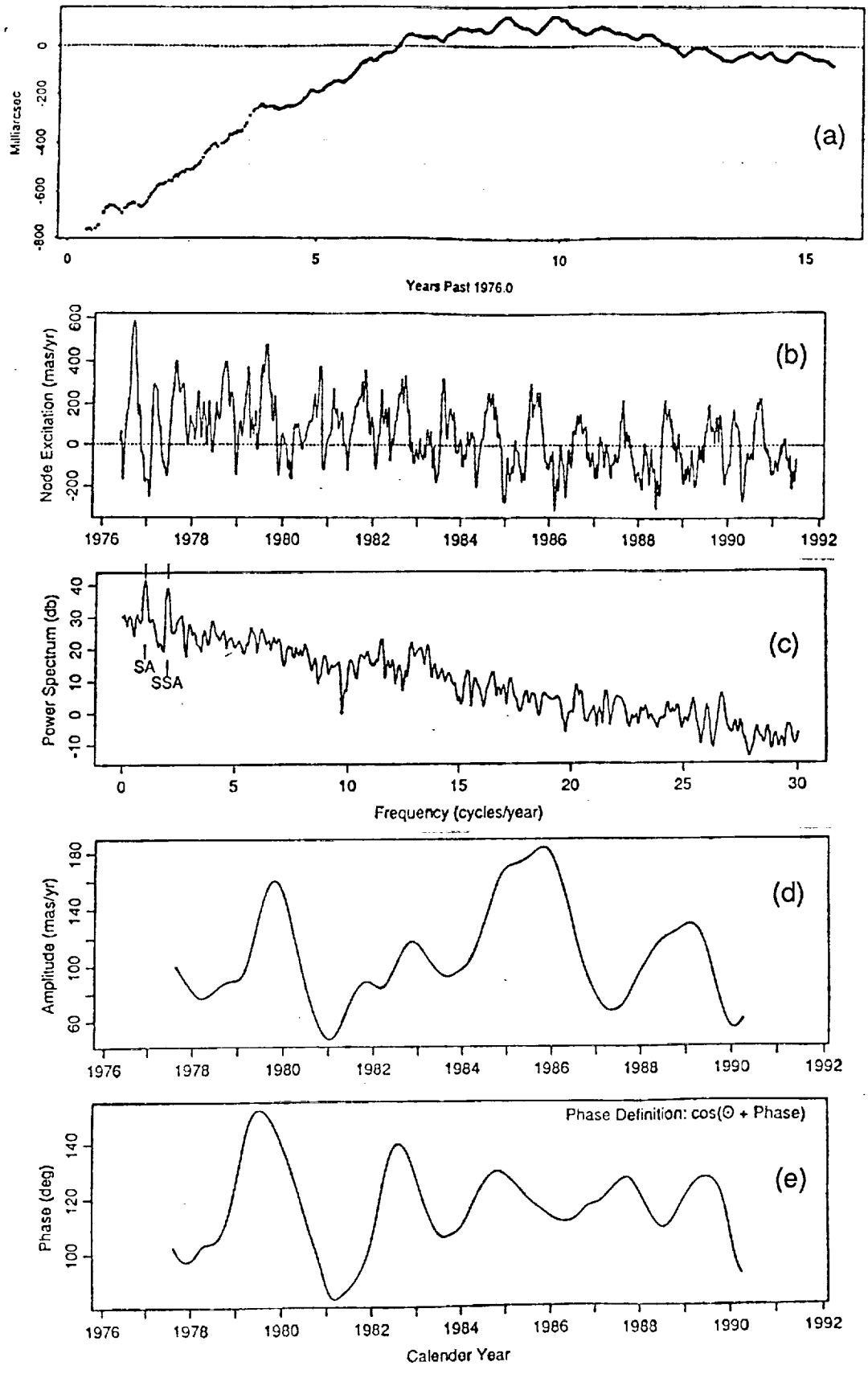
Milliarcsec
0
-200
-400
-600
-800
0
5
10
15
Years Past 1976.0
(a)
Node Excitation (mas/yr)
600
400
200
0
-200
1976
1978
1980
1982
1984
1986
1988
1990
1992
(b)
Power Spectrum (db)
40
30
20
10
0
-10
SA
SSA
0
5
10
15
20
25
30
Frequency (cycles/year)
(c)
Amplitude (mas/yr)
180
140
100
60
1976
1978
1980
1982
1984
1986
1988
1990
1992
(d)
Phase Definition: cos(⊙ + Phase)
Phase (deg)
140
120
100
1976
1978
1980
1982
1984
1986
1988
1990
1992
Calender Year
(e)

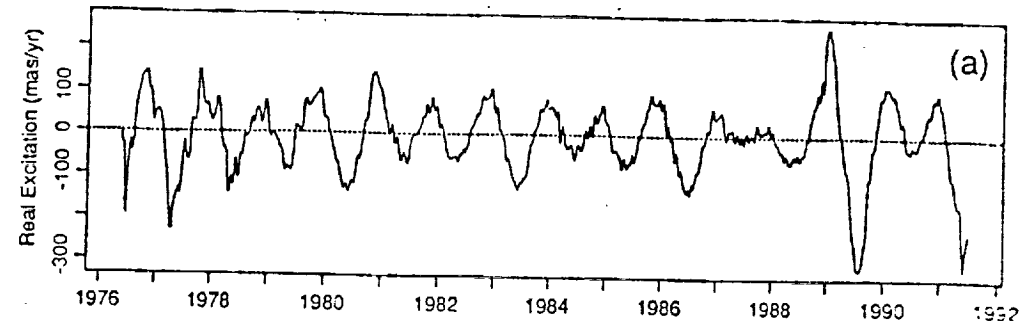
Real Excitation (mas/yr)
-300
-100
0
100
(a)
1976
1978
1980
1982
1984
1986
1988
1990

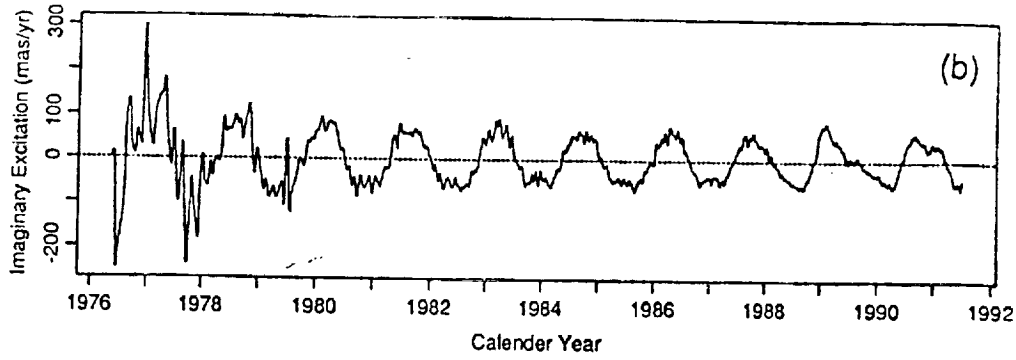
Imaginary Excitation (mas/yr)
-200
0
100
300
(b)
1976
1978
1980
1982
1984
1986
1988
1990
1992
Calender Year

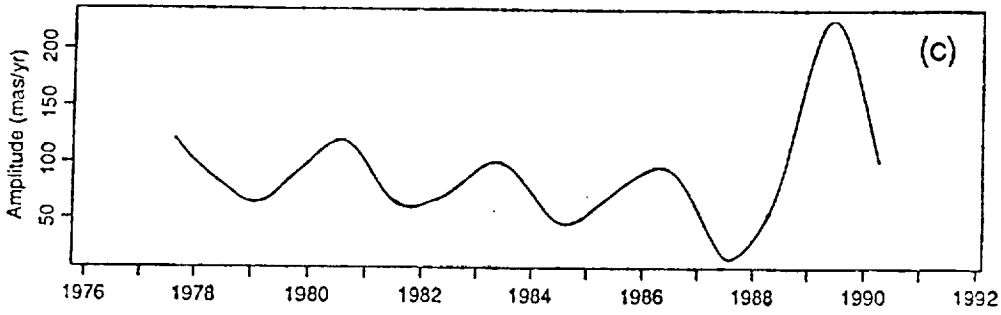
Amplitude (mas/yr)
50
100
150
200
(c)
1976
1978
1980
1982
1984
1986
1988
1990
1992

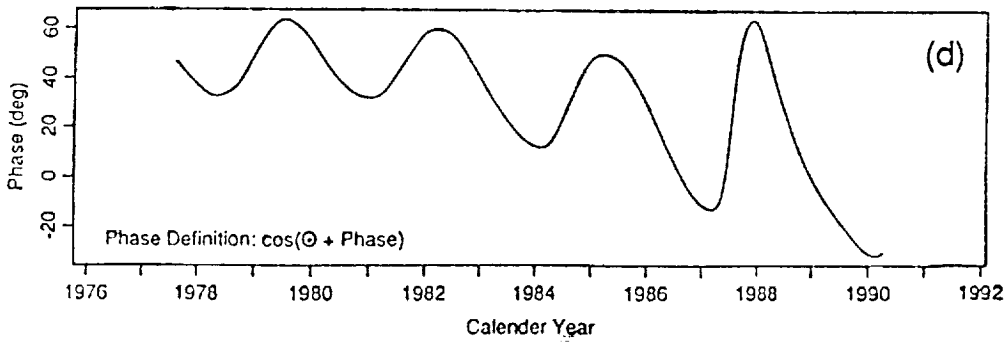
Phase (deg)
-20
0
20
40
60
(d)
Phase Definition: cos(Θ + Phase)
1976
1978
1980
1982
1984
1986
1988
1990
1992
Calender Year

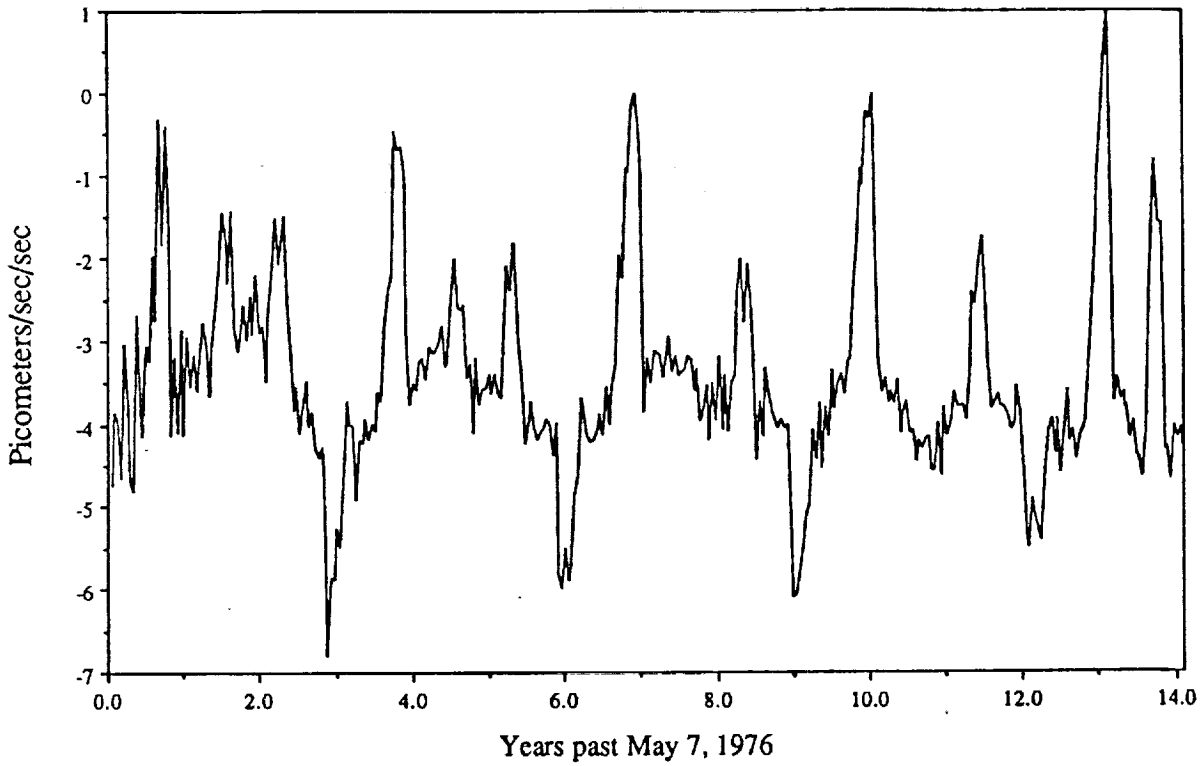

Figure 5. Observed along-track acceleration for Lageos

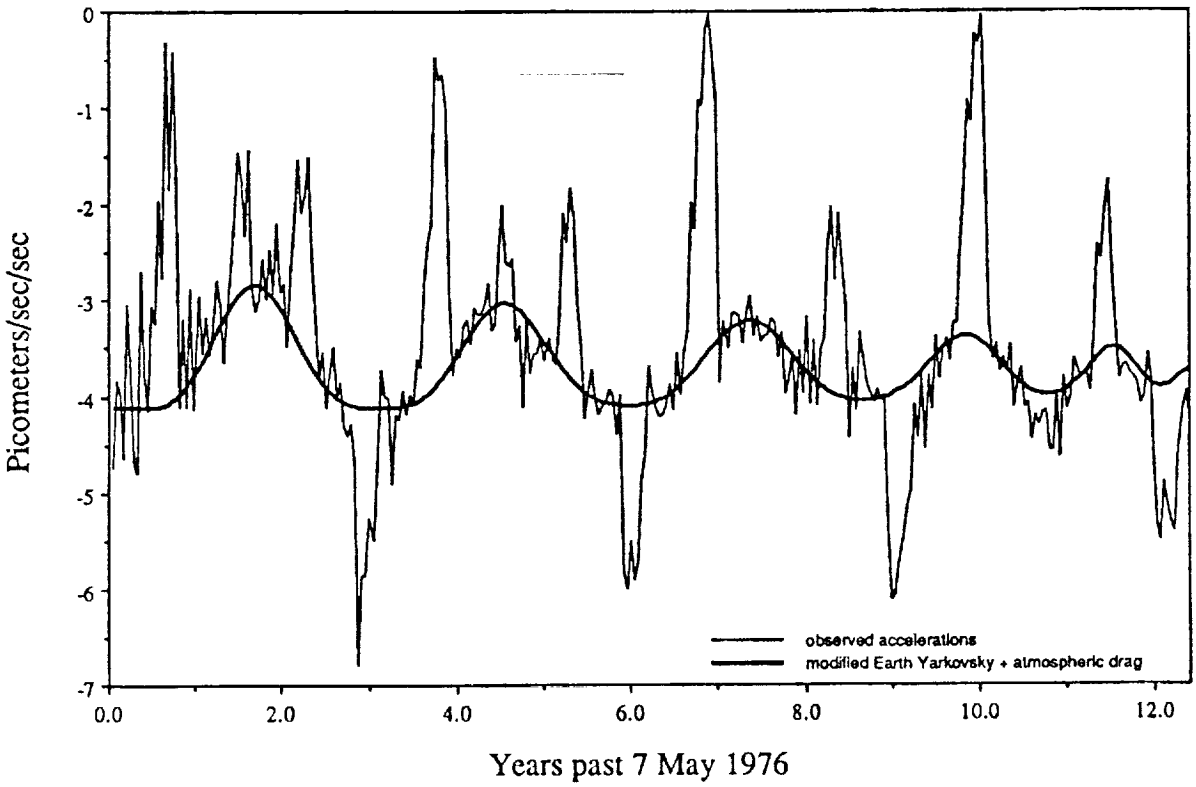

Figure 6. Modified Earth Yarkovsky model compared to observed along-track acceleration during first 12.4 years

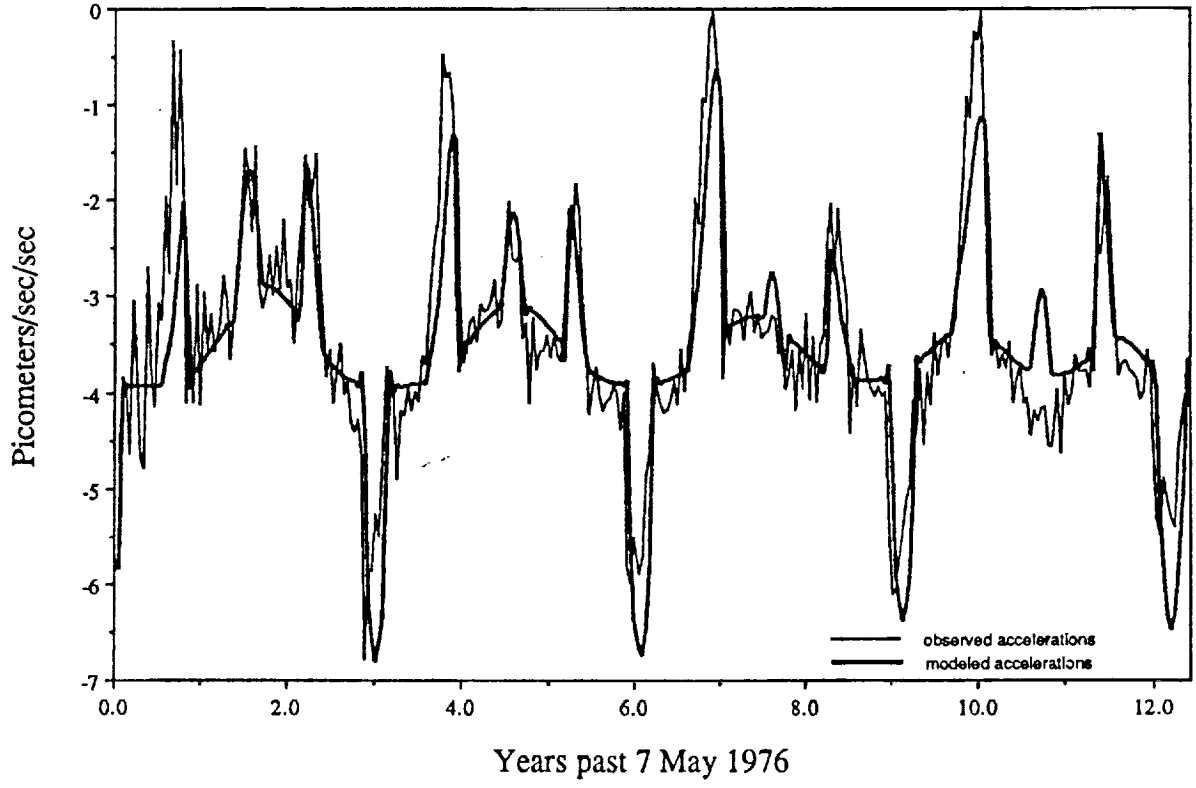

Figure 7. Combined models for Earth and Solar Yarkovsky, asymmetric reflectivity and atmospheric drag compared to observed accelerations

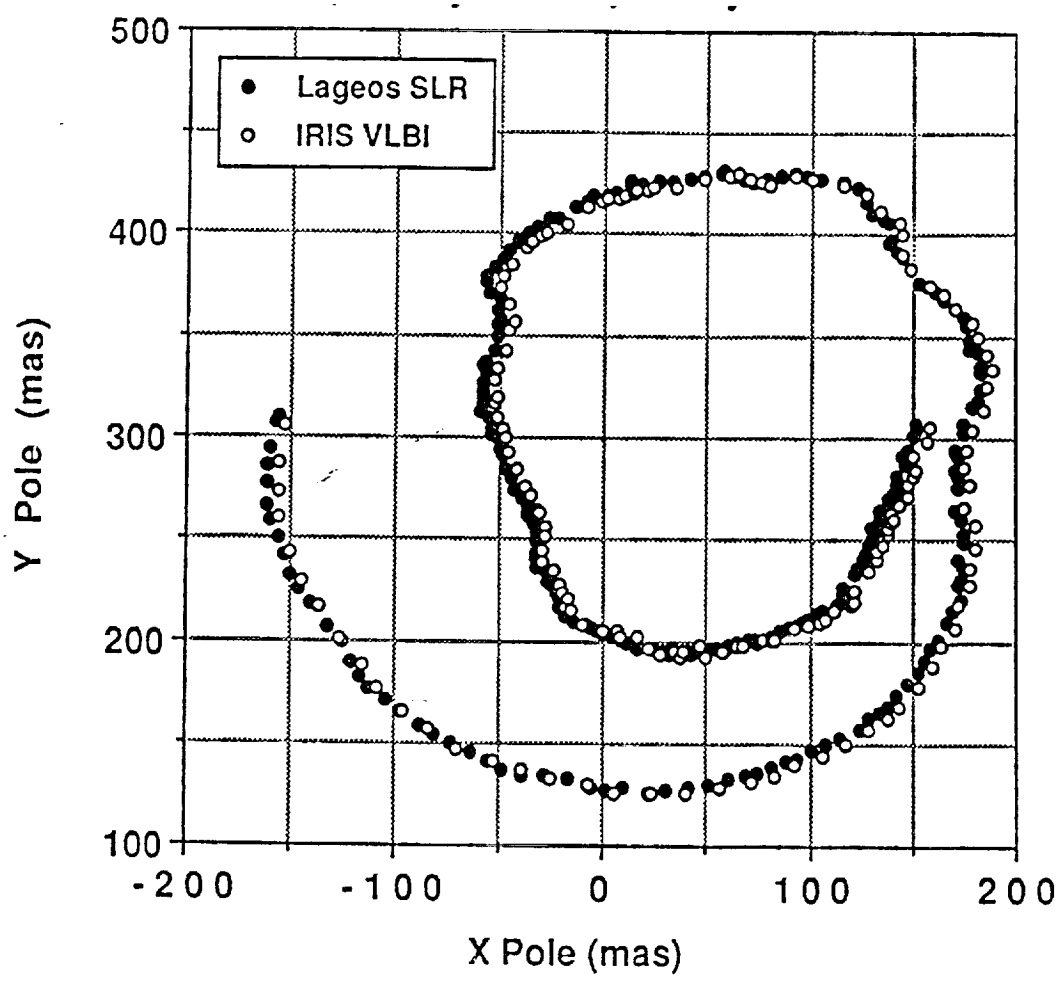

Figure 8. Polhode obtained from UTCSR Lageos and IRIS VLBI, 1987-89

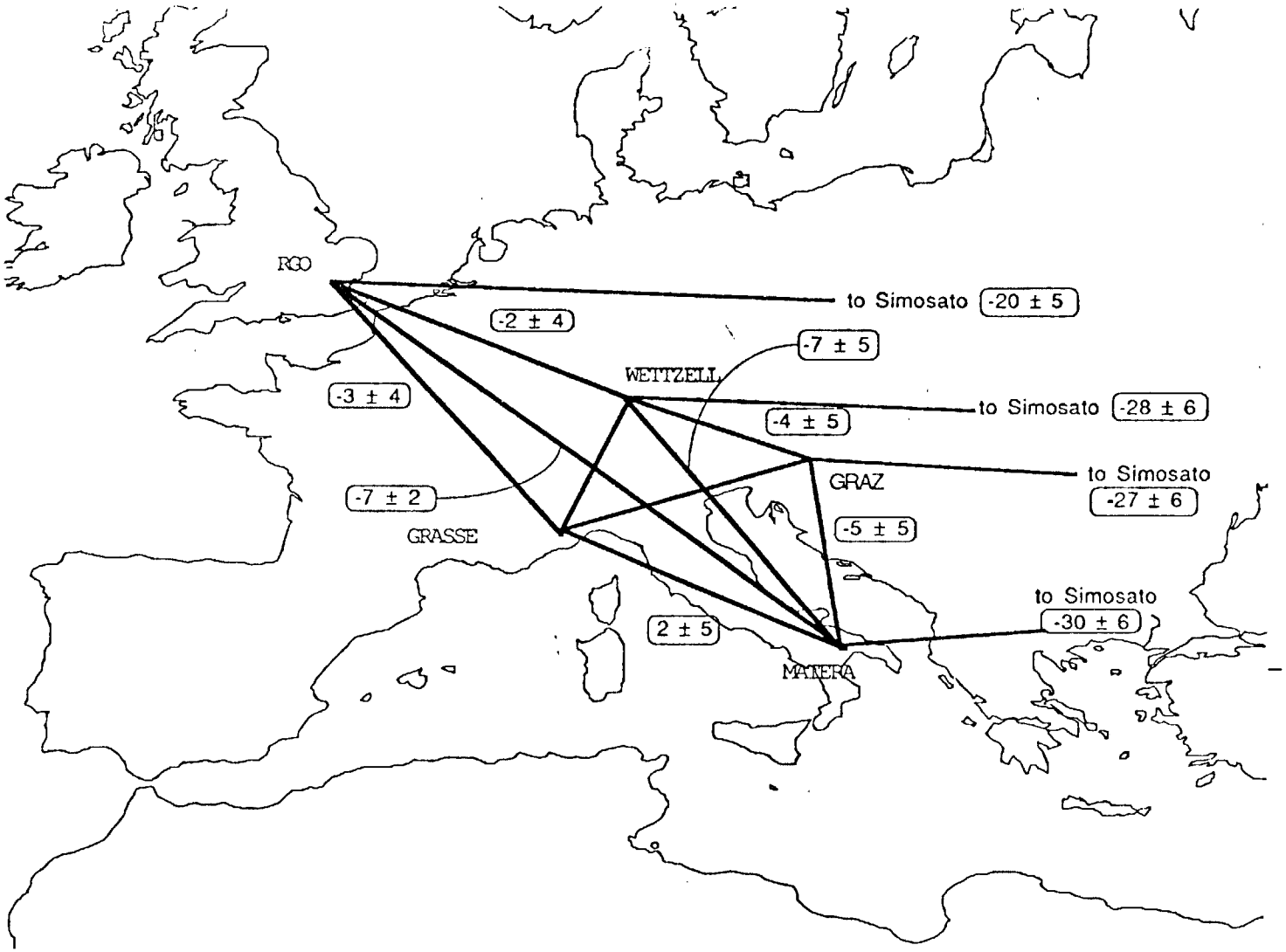

Figure 9. Relative baseline rates for selected European sites

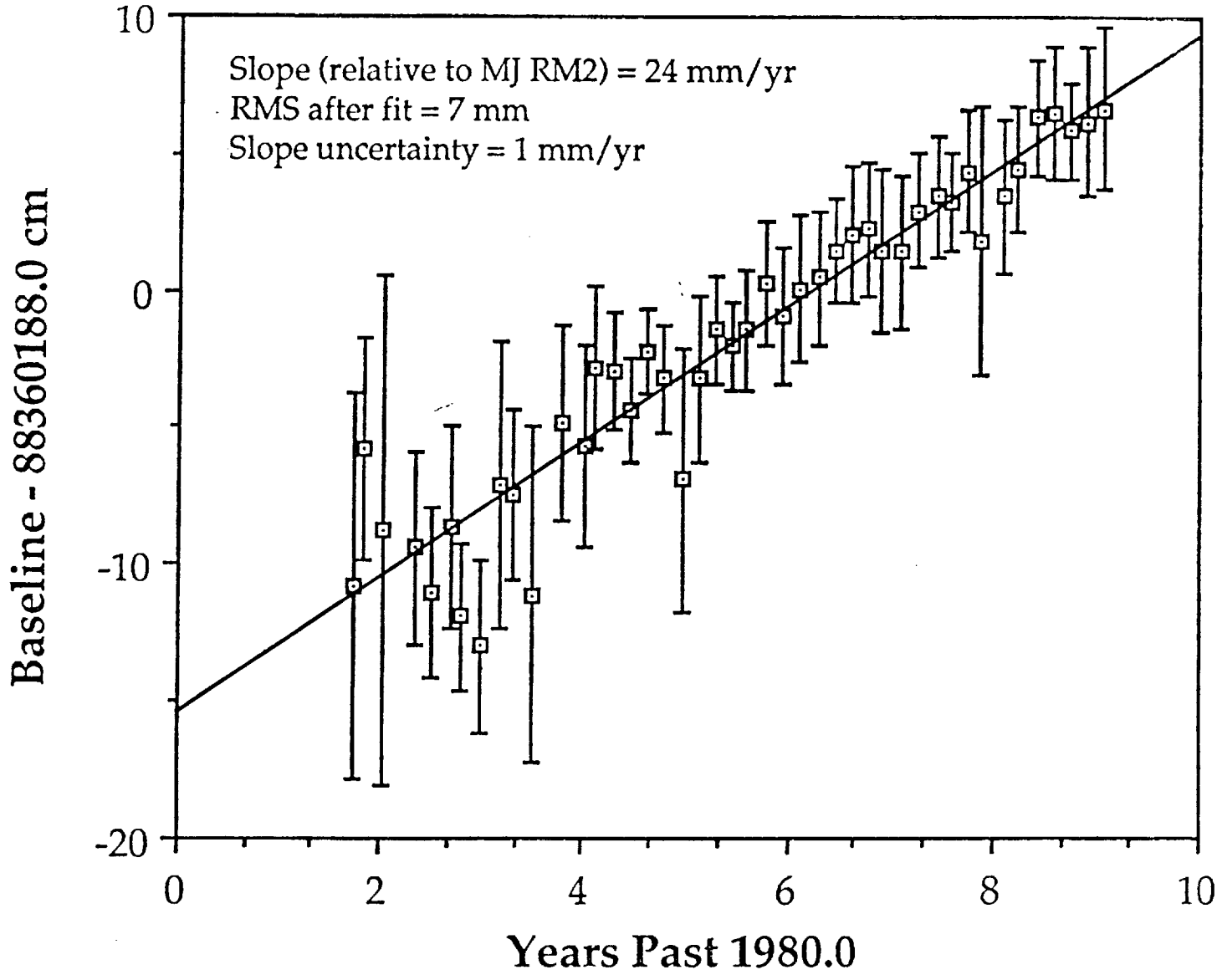

Figure 10. Baseline length variability, Monument Peak to Quincy, 1982-1990

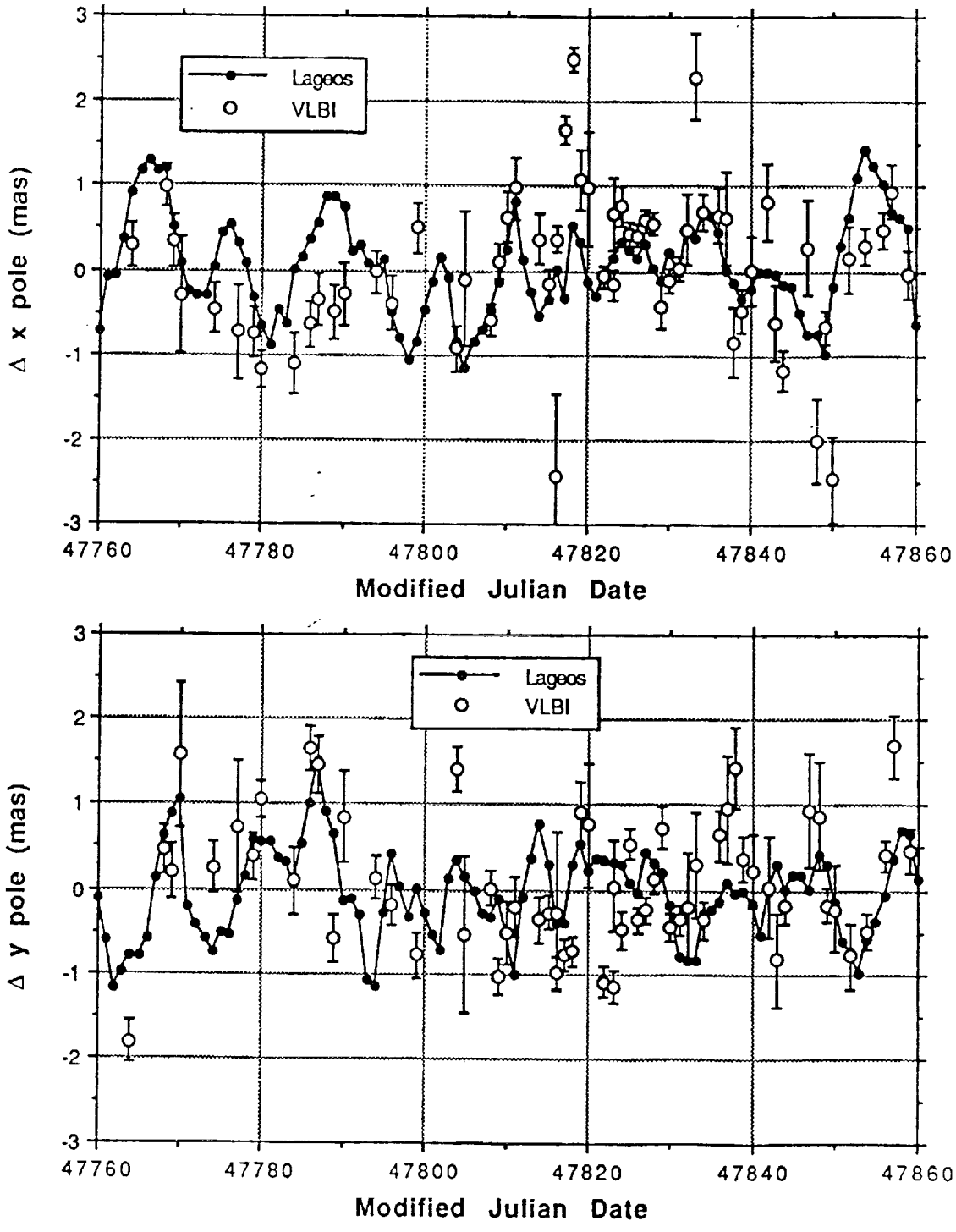

Figure 12. Lageos 1 day Kalman filtered polar motion compared to GSFC VLBI during the 1989 ERDE Campaign